

# Closed-form thermo-mechanical solutions of higher-order theories of cross-ply laminated shallow shells

Rakesh Kumar Khare <sup>a,\*</sup>, Tarun Kant <sup>b</sup>, Ajay Kumar Garg <sup>c</sup>

<sup>a</sup> *Department of Civil Engineering, Shri G. S. Institute of Technology and Science, Indore 452 003, India*

<sup>b</sup> *Department of Civil Engineering, Indian Institute of Technology, Bombay, Powai, Mumbai 400 076, India*

<sup>c</sup> *Department of Civil Engineering, Shri G. S. Institute of Technology and Science, Indore 452 003, India*

---

## Abstract

Closed-form formulations of 2D higher-order shear deformation theories for the thermo-mechanical analysis of simply supported doubly curved cross-ply laminated shells are presented. Formulation includes the Sander's theory for doubly curved shells. Two of the higher-order shear deformation theories account for the effects of both transverse shear strains/stresses and the transverse normal strain/stress, while the third includes only the effects of the transverse shear deformation. In these developments a realistic parabolic distribution of transverse shear strains through the shell thickness is assumed. The temperature variation considered in the formulation is uniform or sinusoidal over the surface and linearly varying through the thickness. Numerical results are presented for thermal and mechanical load cases in laminated composite and sandwich shallow shells. The closed-form solutions presented herein for laminated composite plate or shells are compared with the available 3D elasticity solutions for mechanical loading and it is believed that solutions for thermal loading will serve as bench mark in future.

© 2003 Elsevier Science Ltd. All rights reserved.

*Keywords:* Closed-form solutions; Higher-order theory; Shear deformation; Cross-ply laminates; Thermo-mechanical

---

## 1. Introduction

With the advancement of the technology of composite material it is now possible to use these materials in high-temperature situations. Consequently the thermal deformations and stresses which are induced by non-uniform temperature in composite structures become important parameters in structural design. Use of higher-order theories will make it possible to determine these parameters precisely in composite structures. Studies involving the thermo-elastic behaviour using classical or first-order theories are described by Kant and Khare [1], Khdeir and Reddy [2] and Khdeir et al. [3]. The first ever literature available based on higher-order theory is by Pao [4] who developed higher-order equations applying Flügge's [5] shell theory to orthotropic and laminated materials for the analysis of composite shells under thermal loading. Kant [6,7] presented a general theory for small deformations of a thick shell made up of a layered system of different orthotropic materials having planes of symmetry coincident with the orthogonal reference frame and subjected to mechanical and arbitrary temperature distribution. Kant and Patil [8,9] presented the governing equations describing the behaviour of a general shell form, subjected to both mechanical and thermal loads, specifically for two thick shell theories in addition to a so-called thin shell theory. They considered the numerical examples drawn from literature for the analysis of pressure vessels.

Khdeir and Reddy [2] and Khdeir et al. [3] developed the exact analytical solution of refined plate/shell theories to study the thermal stresses and deformation of cross-ply rectangular plates and cross-ply laminated shallow shells. The state-space approach in conjunction with the Levy method is used to solve exactly the governing equations of the theories under various boundary conditions for plates and doubly curved, cylindrical and spherical shells. Morton and Webber [10] used analytical methods for the calculations of free edge stresses due to mechanical and thermal loads, together with a quadratic interlaminar stress criterion to predict interlaminar failure in laminated composite plates for

---

\* Corresponding author. Tel.: +91-731-537148.

E-mail address: [rakeshkhare@hotmail.com](mailto:rakeshkhare@hotmail.com) (R.K. Khare).

various stacking sequences. Jonnalagadda et al. [11] developed high-order displacement theories for thermoelastic composite plates and compared these with some of the published high-order theories. He [12] used a discrete-layer shear deformation laminated plate theory to analyse steady-state thermal stresses in laminated plates.

Locke [13] developed a numerical Fourier series solution for the classical thin laminated plate equation as applied to inhomogeneous antisymmetric cross-ply laminates subjected to a combined thermal-mechanical load. Dano and Hyer [14] presented a methodology to predict the displacements, particularly the out-of-plane component, of flat unsymmetric epoxy-matrix composite laminates as they are cooled from their elevated temperature. Ali et al. [15] presented a displacement-based higher-order theory, which employs realistic displacement variations. Wang and Karihaloo [16] presented the optimum in situ strength design of multidirectional composite laminates under combined in-plane mechanical and thermal loads. Verijenko et al. [17] developed a higher-order theory of laminated anisotropic shells for the solution of thermal stress problems that takes into account transverse shear stress.

Carrera [18] made a comparative study of theories formulated on the basis of the classical principle of virtual displacements to mixed theories formulated on the basis of the Reissner mixed variational theorem to evaluate the thermal response of orthotropic laminated plates. Zenkour and Fares [19] presented a single-layer thermoelastic model of composite laminated cylindrical shells using a refined first-order theory. Rohwer et al. [20] presented higher-order theories for thermal stresses in layered plates. Patel et al. [21] studied static and dynamic characteristics of thick composite laminates exposed to hygrothermal environment using a realistic higher-order theory. The formulation accounts for the non-linear variation of the in-plane and transverse displacements through the thickness, and abrupt discontinuity in slope of the in-plane displacements at any interface.

The purpose of the present study is to investigate the thermo-mechanical behaviour of simply supported, laminated cross-ply, composite and in particular sandwich shell panels using the various higher-order theories, which account for the effects of transverse shear strains/stresses and the transverse normal strain/stress. In these developments a realistic parabolic distribution of transverse shear strains through the shell thickness is assumed. Analytical solutions are presented to show the effects of variations in geometry, shallowness, lamination parameters and the shear deformation on the thermal response of statically loaded layered anisotropic composite and sandwich shell panels.

## 2. Geometric definition

Fig. 1 contains a differential element of a doubly curved shell. Here  $(x, y, z)$  denote the orthogonal curvilinear coordinates (shell co-ordinates) such that  $x$  and  $y$  curves are lines of principal curvature on the mid-surface  $z = 0$ . The values of the principal radii of curvature of the middle surface are denoted by  $R_x$  and  $R_y$  along  $x$ - and  $y$ -axes respectively.

## 3. Definition of displacement field

The Taylor's series expansion is used to deduce a two-dimensional formulation of a three-dimensional elasticity problem and the following set of equations are obtained by expanding the displacement components  $u(x, y, z)$ ,  $v(x, y, z)$  and  $w(x, y, z)$  of any point in the laminate space in terms of the thickness co-ordinate  $z$ . Thus

$$\begin{aligned} u(x, y, z) &= u_o(x, y) + z\theta_x(x, y) + z^2u_o^*(x, y) + z^3\theta_x^*(x, y), \\ v(x, y, z) &= v_o(x, y) + z\theta_y(x, y) + z^2v_o^*(x, y) + z^3\theta_y^*(x, y), \\ w(x, y, z) &= w_o(x, y) + z\theta_z(x, y) + z^2w_o^*(x, y) + z^3\theta_z^*(x, y). \end{aligned} \quad (1)$$

In the above relations, the terms  $u$ ,  $v$  and  $w$  are the displacements of a general point  $(x, y, z)$  in the laminate domain in the  $x$ ,  $y$  and  $z$  directions respectively. The parameters  $u_o$ ,  $v_o$  are the inplane displacements and  $w_o$  is the transverse displacement of a point  $(x, y)$  on the element middle plane. The functions  $\theta_x$ ,  $\theta_y$  are the rotations of the normal to the element middle plane about  $y$ - and  $x$ -axes respectively, as shown in Fig. 1(a). The parameters  $u_o^*$ ,  $v_o^*$ ,  $w_o^*$ ,  $\theta_x^*$ ,  $\theta_y^*$ ,  $\theta_z^*$  and  $\theta_z$  are the higher-order terms in the Taylor's series expansion and they represent higher-order transverse cross sectional deformation modes.

The various displacement models assumed here for theoretical developments are summarised as follows:

$$\begin{aligned} u &= u_o + z\theta_x + z^2u_o^* + z^3\theta_x^*, \\ v &= v_o + z\theta_y + z^2v_o^* + z^3\theta_y^*, \end{aligned} \quad (2a)$$

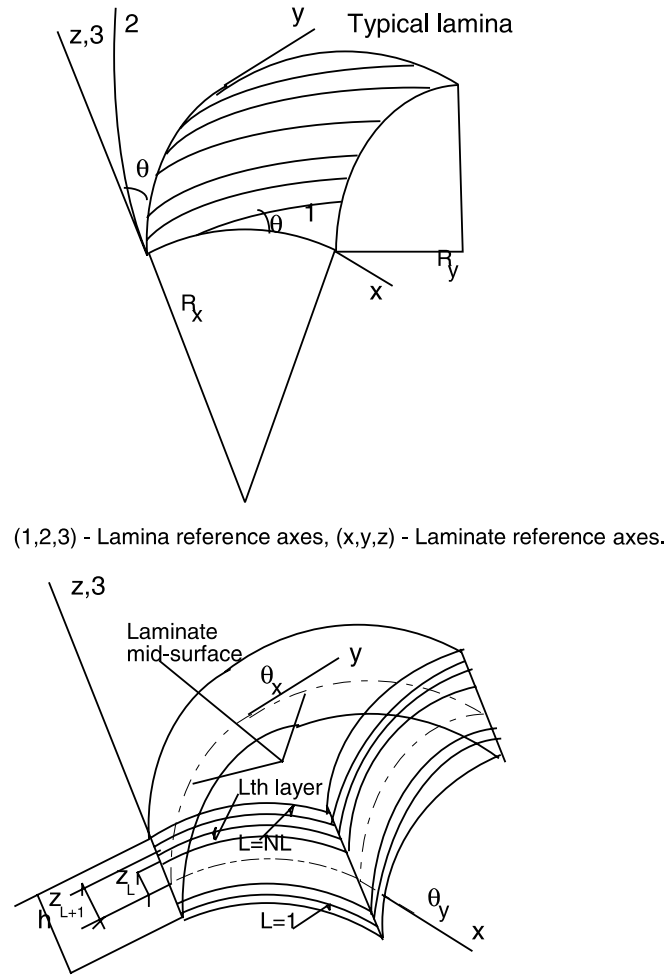


Fig. 1. Laminated shell geometry with positive set of lamina/laminate reference axes, displacement and fibre orientation.

$$\text{HOST12: } w = w_o + z\theta_z + z^2w_o^* + z^3\theta_z^* \tag{2b}$$

$$\text{HOST11: } w = w_o + z\theta_z + z^2w_o^* \tag{2c}$$

$$\text{HOST9: } w = w_o \tag{2d}$$

$$\begin{aligned} \text{FOST: } u &= u_o + z\theta_x, \\ v &= v_o + z\theta_y, \\ w &= w_o. \end{aligned} \tag{2e}$$

#### 4. Strain–displacement relations

With the definition of strains from the linear theory of elasticity, assuming  $h/R_x, h/R_y \ll 1$ , the general strain–displacement relations in the curvilinear co-ordinate system are given as follows:

$$\epsilon_x = \frac{\partial u}{\partial x} + \frac{w}{R_x}, \quad \epsilon_y = \frac{\partial v}{\partial y} + \frac{w}{R_y}, \quad \epsilon_z = \frac{\partial w}{\partial z}, \quad \gamma_{xy} = \frac{\partial u}{\partial y} + \frac{\partial v}{\partial x}, \quad \gamma_{xz} = \frac{\partial u}{\partial z} + \frac{\partial w}{\partial x} - \frac{u}{R_x}, \quad \gamma_{yz} = \frac{\partial v}{\partial z} + \frac{\partial w}{\partial y} - \frac{v}{R_y}. \tag{3}$$

Substituting the expressions for displacements at any point within the laminate space given by Eqs. (2a)–(2e) for the displacement models considered herein, the linear strains in terms of middle surface displacements, for each displacement model can be obtained as follows:

Strain expressions corresponding to model HOST12

$$\begin{aligned}\varepsilon_x &= \varepsilon_{x0} + z\chi_x + z^2\varepsilon_{x0}^* + z^3\chi_x^*, & \varepsilon_y &= \varepsilon_{y0} + z\chi_y + z^2\varepsilon_{y0}^* + z^3\chi_y^*, \\ \varepsilon_z &= \varepsilon_{z0} + z\chi_z^* + z^2\varepsilon_{z0}^*, & \gamma_{xy} &= \varepsilon_{xy0} + z\chi_{xy} + z^2\varepsilon_{xy0}^* + z^3\chi_{xy}^*, \\ \gamma_{xz} &= \phi_x + z\chi_{xz} + z^2\phi_x^* + z^3\chi_{xz}^*, & \gamma_{yz} &= \phi_y + z\chi_{yz} + z^2\phi_y^* + z^3\chi_{yz}^*,\end{aligned}\quad (4a)$$

where

$$\begin{aligned}(\varepsilon_{x0}, \varepsilon_{y0}, \varepsilon_{z0}, \varepsilon_{xy0}) &= \left( \frac{\partial u_o}{\partial x} + \frac{w_o}{R_x}, \frac{\partial v_o}{\partial y} + \frac{w_o}{R_y}, \theta_z, \frac{\partial u_o}{\partial y} + \frac{\partial v_o}{\partial x} \right), \\ (\chi_x, \chi_y, \chi_z^*, \chi_{xy}) &= \left( \frac{\partial \theta_x}{\partial x} + \frac{\theta_z}{R_x}, \frac{\partial \theta_y}{\partial y} + \frac{\theta_z}{R_y}, 2w_o^*, \frac{\partial \theta_y}{\partial x} + \frac{\partial \theta_x}{\partial y} - c_o \frac{\partial v_o}{\partial x} + c_o \frac{\partial u_o}{\partial y} \right), \\ (\varepsilon_{x0}^*, \varepsilon_{y0}^*, \varepsilon_{z0}^*, \varepsilon_{xy0}^*) &= \left( \frac{\partial u_o^*}{\partial x} + \frac{w_o^*}{R_x}, \frac{\partial v_o^*}{\partial y} + \frac{w_o^*}{R_y}, 3\theta_z^*, \frac{\partial u_o^*}{\partial y} + \frac{\partial v_o^*}{\partial x} \right), \\ (\chi_x^*, \chi_y^*, \chi_{xy}^*) &= \left( \frac{\partial \theta_x^*}{\partial x} + \frac{\theta_z^*}{R_x}, \frac{\partial \theta_y^*}{\partial y} + \frac{\theta_z^*}{R_y}, \frac{\partial \theta_x^*}{\partial x} + \frac{\partial \theta_y^*}{\partial y} - c_o \frac{\partial v_o^*}{\partial x} + c_o \frac{\partial u_o^*}{\partial y} \right), \\ (\phi_x, \phi_y, \chi_{xz}, \chi_{yz}) &= \left( \theta_x + \frac{\partial w_o}{\partial x} - \frac{u_o}{R_x}, \theta_y + \frac{\partial w_o}{\partial y} - \frac{v_o}{R_y}, 2u_o^* + \frac{\partial \theta_z}{\partial x} - \frac{\theta_x}{R_x}, 2v_o^* + \frac{\partial \theta_z}{\partial y} - \frac{\theta_y}{R_y} \right), \\ (\phi_x^*, \phi_y^*, \chi_{xz}^*, \chi_{yz}^*) &= \left( 3\theta_x^* + \frac{\partial w_o^*}{\partial x} - \frac{u_o^*}{R_x}, 3\theta_y^* + \frac{\partial w_o^*}{\partial y} - \frac{v_o^*}{R_y}, \frac{\partial \theta_z^*}{\partial x} - \frac{\theta_x^*}{R_x}, \frac{\partial \theta_z^*}{\partial y} - \frac{\theta_y^*}{R_y} \right)\end{aligned}\quad (4b)$$

in which,  $c_o$  denotes the constant

$$c_o = \frac{1}{2} \left( \frac{1}{R_x} - \frac{1}{R_y} \right). \quad (4c)$$

This term is introduced by Sanders [22] and distinguishes the Sander's theory from others. The strain expressions corresponding to the displacement models of other higher-order theories are same as of displacement model HOST12 with following difference.

HOST11

$$\varepsilon_z = \varepsilon_{z0} + z\chi_z^*, \quad (\chi_x^*, \chi_y^*) = \left( \frac{\partial \theta_x^*}{\partial x}, \frac{\partial \theta_y^*}{\partial y} \right), \quad (\chi_{xz}^*, \chi_{yz}^*) = \left( -\frac{\theta_x^*}{R_x}, -\frac{\theta_y^*}{R_y} \right). \quad (4d)$$

HOST9

$$\begin{aligned}\varepsilon_z &= 0, \quad (\chi_x, \chi_y) = \left( \frac{\partial \theta_x}{\partial x}, \frac{\partial \theta_y}{\partial y} \right), \quad (\varepsilon_{x0}^*, \varepsilon_{y0}^*) = \left( \frac{\partial u_o^*}{\partial x}, \frac{\partial v_o^*}{\partial y} \right), \\ (\chi_x^*, \chi_y^*) &= \left( \frac{\partial \theta_x^*}{\partial x}, \frac{\partial \theta_y^*}{\partial y} \right), \quad (\chi_{xz}, \chi_{yz}) = \left( 2u_o^* - \frac{\theta_x}{R_x}, 2v_o^* - \frac{\theta_y}{R_y} \right), \\ (\phi_x^*, \phi_y^*, \chi_{xz}^*, \chi_{yz}^*) &= \left( 3\theta_x^* - \frac{u_o^*}{R_x}, 3\theta_y^* - \frac{v_o^*}{R_y}, -\frac{\theta_x^*}{R_x}, -\frac{\theta_y^*}{R_y} \right).\end{aligned}\quad (4e)$$

FOST

$$\begin{aligned}\varepsilon_x &= \varepsilon_{x0} + z\chi_x, \quad \varepsilon_y = \varepsilon_{y0} + z\chi_y, \quad \varepsilon_z = 0, \\ \gamma_{xy} &= \varepsilon_{xy0} + z\chi_{xy}, \quad \gamma_{xz} = \phi_x + z\chi_{xz}, \quad \gamma_{yz} = \phi_y + z\chi_{yz},\end{aligned}\quad (4f)$$

where all above terms are same as given in displacement model HOST9, except following terms:

$$(\chi_{xz}, \chi_{yz}) = \left( -\frac{\theta_x}{R_x}, -\frac{\theta_y}{R_y} \right). \quad (4g)$$

## 5. Stress–strain relations and stress resultants

Assuming the principal material axes (1, 2, 3) and laminate axes (x, y, z) in the curvilinear co-ordinate system as defined in Fig. 1, the three-dimensional stress–strain relations for an orthotropic lamina with reference to the principal material axes for the theory to be developed based on the displacement model HOST12 and HOST11 are defined as follows:

$$\begin{Bmatrix} \sigma_1 \\ \sigma_2 \\ \sigma_3 \\ \tau_{12} \\ \tau_{13} \\ \tau_{23} \end{Bmatrix}^L = \begin{bmatrix} C_{11} & C_{12} & C_{13} & 0 & 0 & 0 \\ C_{12} & C_{22} & C_{23} & 0 & 0 & 0 \\ C_{13} & C_{23} & C_{33} & 0 & 0 & 0 \\ 0 & 0 & 0 & C_{44} & 0 & 0 \\ 0 & 0 & 0 & 0 & C_{55} & 0 \\ 0 & 0 & 0 & 0 & 0 & C_{66} \end{bmatrix}^L \begin{Bmatrix} \varepsilon_1 - \alpha_1 \Delta T \\ \varepsilon_2 - \alpha_2 \Delta T \\ \varepsilon_3 - \alpha_3 \Delta T \\ \gamma_{12} \\ \gamma_{13} \\ \gamma_{23} \end{Bmatrix}^L \quad (5a)$$

in which

$$\begin{aligned} C_{11} &= \frac{E_1(1 - \nu_{23}\nu_{32})}{\nu^*}, & C_{12} &= \frac{E_1(\nu_{21} + \nu_{31}\nu_{23})}{\nu^*}, \\ C_{13} &= \frac{E_1(\nu_{31} + \nu_{21}\nu_{32})}{\nu^*}, & C_{22} &= \frac{E_2(1 - \nu_{13}\nu_{31})}{\nu^*}, \\ C_{23} &= \frac{E_2(\nu_{32} + \nu_{12}\nu_{31})}{\nu^*}, & C_{33} &= \frac{E_3(1 - \nu_{12}\nu_{21})}{\nu^*}, \\ C_{44} &= G_{12}, & C_{55} &= G_{13}, & C_{66} &= G_{23}, \\ \nu^* &= (1 - \nu_{12}\nu_{21} - \nu_{23}\nu_{32} - \nu_{31}\nu_{13} - 2\nu_{21}\nu_{32}\nu_{13}). \end{aligned} \quad (5b)$$

Here  $\Delta T$  is the temperature rise and  $\alpha_i$  ( $i = 1, 2, 3$ ) are the linear thermal expansion coefficients in the directions of principal material axes.  $E$ 's and  $\nu$ 's are Young's moduli and Poisson's ratios, which are not independent but related by the expressions:

$$\frac{\nu_{12}}{E_1} = \frac{\nu_{21}}{E_2}, \quad \frac{\nu_{13}}{E_1} = \frac{\nu_{31}}{E_3} \quad \text{and} \quad \frac{\nu_{23}}{E_2} = \frac{\nu_{32}}{E_3}. \quad (5c)$$

In conformity with the assumptions that the normal stress  $\sigma_3$  may be assumed small and negligible and the corresponding strain  $\varepsilon_3$  is equal to zero. Eqs. (5a)–(5c) is modified and the corresponding reduced stress–strain relations are given as

$$\begin{Bmatrix} \sigma_1 \\ \sigma_2 \\ \tau_{12} \\ \tau_{13} \\ \tau_{23} \end{Bmatrix}^L = \begin{bmatrix} \bar{C}_{11} & \bar{C}_{12} & 0 & 0 & 0 \\ \bar{C}_{12} & \bar{C}_{22} & 0 & 0 & 0 \\ 0 & 0 & \bar{C}_{33} & 0 & 0 \\ 0 & 0 & 0 & \bar{C}_{44} & 0 \\ 0 & 0 & 0 & 0 & \bar{C}_{55} \end{bmatrix}^L \begin{Bmatrix} \varepsilon_1 - \alpha_1 \Delta T \\ \varepsilon_2 - \alpha_2 \Delta T \\ \gamma_{12} \\ \gamma_{13} \\ \gamma_{23} \end{Bmatrix}^L, \quad (6a)$$

where

$$\begin{aligned} \bar{C}_{11} &= E_1/(1 - \nu_{12}\nu_{21}), & \bar{C}_{12} &= \nu_{21}E_1/(1 - \nu_{12}\nu_{21}), \\ \bar{C}_{22} &= E_2/(1 - \nu_{12}\nu_{21}), & \nu_{12}/E_1 &= \nu_{21}/E_2, \\ \bar{C}_{33} &= G_{12}, & \bar{C}_{44} &= G_{13}, & \bar{C}_{55} &= G_{23}. \end{aligned} \quad (6b)$$

The relations given by Eqs. (6a) and (6b) are adopted to develop theoretical formulation based on the displacement models HOST9 and FOST.

These equations in compacted form may be written as

$$\sigma' = C\varepsilon'. \quad (7)$$

As mentioned earlier, the relations given by Eq. (7) are the stress–strain constitutive relations for the  $L$ th orthotropic lamina referred to lamina's principal material axes (1, 2, 3). The principal material axes of lamina may not coincide with the reference axes of the laminate ( $x, y, z$ ) (refer Fig. 1). It is therefore necessary to transform the constitutive relations from the lamina fibre axes (1, 2, 3) to laminate reference axes ( $x, y, z$ ). This is conveniently accomplished through the transformations as described by Cook [23]. The final relations are as follows:

$$\begin{Bmatrix} \sigma_x \\ \sigma_y \\ \sigma_z \\ \tau_{xy} \\ \tau_{xz} \\ \tau_{yz} \end{Bmatrix} = \begin{bmatrix} Q_{11} & Q_{12} & Q_{13} & Q_{14} & 0 & 0 \\ Q_{12} & Q_{22} & Q_{23} & Q_{24} & 0 & 0 \\ Q_{13} & Q_{23} & Q_{33} & Q_{34} & 0 & 0 \\ Q_{14} & Q_{24} & Q_{34} & Q_{44} & 0 & 0 \\ 0 & 0 & 0 & 0 & Q_{55} & Q_{56} \\ 0 & 0 & 0 & 0 & Q_{56} & Q_{66} \end{bmatrix} \begin{Bmatrix} \varepsilon_x - \alpha_x \Delta T \\ \varepsilon_y - \alpha_y \Delta T \\ \varepsilon_z - \alpha_z \Delta T \\ \gamma_{xy} - \alpha_{xy} \Delta T \\ \gamma_{xz} \\ \gamma_{yz} \end{Bmatrix}, \quad (8a)$$

where

$$\begin{aligned}\alpha_x &= \alpha_1 \cos^2 \theta + \alpha_2 \sin^2 \theta, \\ \alpha_y &= \alpha_1 \sin^2 \theta + \alpha_2 \cos^2 \theta, \\ \alpha_z &= \alpha_3, \\ \alpha_{xy} &= 2(\alpha_1 - \alpha_2) \sin \theta \cos \theta.\end{aligned}\quad (8b)$$

In the above equations  $\theta$  is the angle of the axis parallel to the fibres (direction-1) with the  $x$ -axis. Similarly the stress-strain relations of the  $L$ th lamina for the theory to be developed based on displacement model HOST9 and FOST are as follows:

$$\begin{Bmatrix} \sigma_x \\ \sigma_y \\ \tau_{xy} \\ \tau_{xz} \\ \tau_{yz} \end{Bmatrix} = \begin{bmatrix} \bar{Q}_{11} & \bar{Q}_{12} & \bar{Q}_{13} & 0 & 0 \\ \bar{Q}_{12} & \bar{Q}_{22} & \bar{Q}_{23} & 0 & 0 \\ \bar{Q}_{13} & \bar{Q}_{23} & \bar{Q}_{33} & 0 & 0 \\ 0 & 0 & 0 & \bar{Q}_{44} & \bar{Q}_{45} \\ 0 & 0 & 0 & \bar{Q}_{45} & \bar{Q}_{55} \end{bmatrix} \begin{Bmatrix} \varepsilon_x - \alpha_x \Delta T \\ \varepsilon_y - \alpha_y \Delta T \\ \gamma_{xy} - \alpha_{xy} \Delta T \\ \gamma_{xz} \\ \gamma_{yz} \end{Bmatrix}\quad (8c)$$

or in concise form

$$\bar{\sigma} = \mathbf{Q} \bar{\varepsilon} \quad (9)$$

in which the coefficients of the  $\mathbf{Q}$  matrix, called as reduced elastic constants of the orthotropic material corresponding to  $L$ th lamina are defined in Appendix A. Upon integrating through the laminate thickness the Eq. (9) is reduced to

$$\bar{\sigma} = \mathbf{D} \bar{\varepsilon} - \mathbf{N}_T \quad (10a)$$

$$\text{in which } \mathbf{D} = \begin{bmatrix} \mathbf{D}_f & 0 \\ 0 & \mathbf{D}_s \end{bmatrix}, \quad \text{where } \mathbf{D}_f = \begin{bmatrix} \mathbf{D}_m & \mathbf{D}_c \\ \mathbf{D}_c^t & \mathbf{D}_b \end{bmatrix}. \quad (10b)$$

$\bar{\varepsilon}$  and  $\bar{\sigma}$  are the vectors of mid-surface strains and stress resultants respectively,  $\mathbf{N}_T$  is the vector of thermal stress resultants corresponding to  $\bar{\sigma}$  and the matrices  $\mathbf{D}_m$ ,  $\mathbf{D}_b$ ,  $\mathbf{D}_c$  and  $\mathbf{D}_s$  for various displacement models are given in Appendix B. The component of the mid-surface strain vector  $\bar{\varepsilon}$  and the corresponding components of the stress-resultant vector  $\bar{\sigma}$  and the thermal stress-resultant vector  $\mathbf{N}_T$  for various models are defined as follows:

For displacement models HOST12 and HOST11

$$\bar{\sigma} = (N_x, N_y, N_{xy}, N_x^*, N_y^*, N_{xy}^*, N_z, N_z^*, M_x, M_y, M_{xy}, M_x^*, M_y^*, M_{xy}^*, M_z^*, Q_x, Q_y, Q_x^*, Q_y^*, S_x, S_y, S_x^*, S_y^*)^t, \quad (11a)$$

$$\bar{\varepsilon} = (\varepsilon_{x0}, \varepsilon_{y0}, \varepsilon_{xy0}, \varepsilon_{x0}^*, \varepsilon_{y0}^*, \varepsilon_{xy0}^*, \varepsilon_{z0}, \varepsilon_{z0}^*, \chi_x, \chi_y, \chi_{xy}, \chi_x^*, \chi_y^*, \chi_{xy}^*, \chi_z^*, \phi_x, \phi_y, \phi_x^*, \phi_y^*, \chi_{xz}, \chi_{yz}, \chi_{xz}^*, \chi_{yz}^*)^t, \quad (11b)$$

$$\mathbf{N}_T = (N_{xT}, N_{yT}, N_{xyT}, N_{xT}^*, N_{yT}^*, N_{xyT}^*, N_{zT}, N_{zT}^*, M_{xT}, M_{yT}, M_{xyT}, M_{xT}^*, M_{yT}^*, M_{xyT}^*, M_{zT}, 0, 0, 0, 0, 0, 0, 0, 0)^t, \quad (11c)$$

where the components of the stress-resultants vector  $\bar{\sigma}$  for the laminate with NL number of layers are defined as

$$\begin{bmatrix} N_x & N_x^* & M_x & M_x^* \\ N_y & N_y^* & M_y & M_y^* \\ N_z & N_z^* & M_z & 0 \\ N_{xy} & N_{xy}^* & M_{xy} & M_{xy}^* \end{bmatrix} = \sum_{L=1}^{NL} \int_{Z_L}^{Z_{L+1}} \begin{Bmatrix} \varepsilon_x \\ \varepsilon_y \\ \varepsilon_z \\ \gamma_{xy} \end{Bmatrix} (1, z^2, z, z^3) dz \quad (12a)$$

$$= \sum_{L=1}^{NL} \int_{Z_L}^{Z_{L+1}} \begin{bmatrix} Q_{11} & Q_{12} & Q_{13} & Q_{14} \\ Q_{12} & Q_{22} & Q_{23} & Q_{24} \\ Q_{13} & Q_{23} & Q_{33} & Q_{34} \\ Q_{14} & Q_{24} & Q_{34} & Q_{44} \end{bmatrix} \begin{Bmatrix} \varepsilon_x \\ \varepsilon_y \\ \varepsilon_z \\ \gamma_{xy} \end{Bmatrix} (1, z^2, z, z^3) dz - \begin{bmatrix} N_{xT} & N_{xT}^* & M_{xT} & M_{xT}^* \\ N_{yT} & N_{yT}^* & M_{yT} & M_{yT}^* \\ N_{zT} & N_{zT}^* & M_{zT} & 0 \\ N_{xyT} & N_{xyT}^* & M_{xyT} & M_{xyT}^* \end{bmatrix}, \quad (12b)$$

$$\begin{bmatrix} Q_x & Q_x^* & S_x & S_x^* \\ Q_y & Q_y^* & S_y & S_y^* \end{bmatrix} = \sum_{L=1}^{NL} \int_{Z_L}^{Z_{L+1}} \begin{Bmatrix} \tau_{xz} \\ \tau_{yz} \end{Bmatrix} (1, z^2, z, z^3) dz \quad (12c)$$

and the thermal stress resultants are defined as

$$\begin{bmatrix} N_{xT} & N_{xT}^* & M_{xT} & M_{xT}^* \\ N_{yT} & N_{yT}^* & M_{yT} & M_{yT}^* \\ N_{zT} & N_{zT}^* & M_{zT} & 0 \\ N_{xyT} & N_{xyT}^* & M_{xyT} & M_{xyT}^* \end{bmatrix} = \sum_{L=1}^{NL} \int_{Z_L}^{Z_{L+1}} \begin{bmatrix} Q_{11} & Q_{12} & Q_{13} & Q_{14} \\ Q_{12} & Q_{22} & Q_{23} & Q_{24} \\ Q_{13} & Q_{23} & Q_{33} & Q_{34} \\ Q_{14} & Q_{24} & Q_{34} & Q_{44} \end{bmatrix} \begin{Bmatrix} \alpha_x \\ \alpha_y \\ \alpha_z \\ \alpha_{xy} \end{Bmatrix} \Delta T (1, z^2, z, z^3) dz. \quad (12d)$$

To use the same flexural rigidity matrix as is used in displacement model HOST12 defined above the terms  $N_z^* = 0$  and  $\varepsilon_z^* = 0$  are retained in the displacement model HOST11 with zero values so that they are not effecting the equilibrium equations.

For displacement model HOST9

$$\bar{\sigma} = (N_x, N_y, N_{xy}, N_x^*, N_y^*, N_{xy}^*, M_x, M_y, M_{xy}, M_x^*, M_y^*, M_{xy}^*, Q_x, Q_y, Q_x^*, Q_y^*, S_x, S_y, S_x^*, S_y^*)^t, \quad (13a)$$

$$\bar{\varepsilon} = (\varepsilon_{x0}, \varepsilon_{y0}, \varepsilon_{xy0}, \varepsilon_{x0}^*, \varepsilon_{y0}^*, \varepsilon_{xy0}^*, \gamma_x, \gamma_y, \gamma_{xy}, \gamma_x^*, \gamma_y^*, \gamma_{xy}^*, \phi_x, \phi_y, \phi_x^*, \phi_y^*, \gamma_{xz}, \gamma_{yz}, \gamma_{xz}^*, \gamma_{yz}^*)^t, \quad (13b)$$

$$\mathbf{N}_T = (N_{xT}, N_{yT}, N_{xyT}, N_{xT}^*, N_{yT}^*, N_{xyT}^*, M_{xT}, M_{yT}, M_{xyT}, M_{xT}^*, M_{yT}^*, M_{xyT}^*, 0, 0, 0, 0, 0, 0)^t. \quad (13c)$$

For displacement model FOST

$$\bar{\sigma} = (N_x, N_y, N_{xy}, M_x, M_y, M_{xy}, Q_x, Q_y, S_x, S_y)^t, \quad (14a)$$

$$\bar{\varepsilon} = (\varepsilon_{x0}, \varepsilon_{y0}, \varepsilon_{xy0}, \gamma_x, \gamma_y, \gamma_{xy}, \phi_x, \phi_y, \gamma_{xz}, \gamma_{yz})^t, \quad (14b)$$

$$\mathbf{N}_T = (N_{xT}, N_{yT}, N_{xyT}, M_{xT}, M_{yT}, M_{xyT}, 0, 0, 0, 0)^t. \quad (14c)$$

The definition of components of the vectors of stress-resultants  $\bar{\sigma}$  and the thermal stress resultants  $\mathbf{N}_T$  for the element laminate with NL number of layers is same as given in Eqs. (12a)–(12d) with corresponding reduced elastic constants.

## 6. Equilibrium equations and boundary conditions

For equilibrium, the total potential energy must be stationary and using the definitions of stress-resultants and mid-surface strains stated in above sections principal of virtual work yields

$$\delta\Pi = \delta(U - W) = 0, \quad (15)$$

where  $U$  is the strain energy of the laminate and  $W$  represents the work done by external forces. These are evaluated as follows:

$$\delta U = \int_x \int_y \int_z (\sigma_x \delta \varepsilon_x + \sigma_y \delta \varepsilon_y + \sigma_z \delta \varepsilon_z + \tau_{xy} \delta \gamma_{xy} + \tau_{xz} \delta \gamma_{xz} + \tau_{yz} \delta \gamma_{yz}) dx dy dz. \quad (16)$$

Integration through the plate thickness and substituting in terms of mid-surface strains and introducing stress resultants, the above relations transform in the following form.

For displacement model HOST12 and HOST11

$$\begin{aligned} \delta\Pi = \int_x \int_y (N_x \delta \varepsilon_{x0} + N_y \delta \varepsilon_{y0} + N_{xy} \delta \varepsilon_{xy0} + N_x^* \delta \varepsilon_{x0}^* + N_y^* \delta \varepsilon_{y0}^* + N_{xy}^* \delta \varepsilon_{xy0}^* + N_z \delta \varepsilon_{z0} + N_z^* \delta \varepsilon_{z0}^* + M_x \delta \gamma_x + M_y \delta \gamma_y + M_{xy} \delta \gamma_{xy} \\ + M_x^* \delta \gamma_x^* + M_y^* \delta \gamma_y^* + M_{xy}^* \delta \gamma_{xy}^* + M_z \delta \gamma_z^* + Q_x \delta \phi_x + Q_y \delta \phi_y + Q_x^* \delta \phi_x^* + Q_y^* \delta \phi_y^* + S_x \delta \gamma_{xz} + S_y \delta \gamma_{yz} + S_x^* \delta \gamma_{xz}^* \\ + S_y^* \delta \gamma_{yz}^* - \delta w_o q) dx dy = 0. \end{aligned} \quad (17a)$$

For displacement model HOST9

$$\begin{aligned} \delta\Pi = \int_x \int_y (N_x \delta \varepsilon_{x0} + N_y \delta \varepsilon_{y0} + N_{xy} \delta \varepsilon_{xy0} + N_x^* \delta \varepsilon_{x0}^* + N_y^* \delta \varepsilon_{y0}^* + N_{xy}^* \delta \varepsilon_{xy0}^* + M_x \delta \gamma_x + M_y \delta \gamma_y + M_{xy} \delta \gamma_{xy} + M_x^* \delta \gamma_x^* \\ + M_y^* \delta \gamma_y^* + M_{xy}^* \delta \gamma_{xy}^* + Q_x \delta \phi_x + Q_y \delta \phi_y + Q_x^* \delta \phi_x^* + Q_y^* \delta \phi_y^* + S_x \delta \gamma_{xz} + S_y \delta \gamma_{yz} - \delta w_o q) dx dy = 0. \end{aligned} \quad (17b)$$

For displacement model FOST

$$\begin{aligned} \delta\Pi = \int_x \int_y (N_x \delta \varepsilon_{x0} + N_y \delta \varepsilon_{y0} + N_{xy} \delta \varepsilon_{xy0} + M_x \delta \gamma_x + M_y \delta \gamma_y + M_{xy} \delta \gamma_{xy} + Q_x \delta \phi_x + Q_y \delta \phi_y + S_x \delta \gamma_{xz} + S_y \delta \gamma_{yz} \\ - \delta w_o q) dx dy = 0 \end{aligned} \quad (17c)$$

in the above equations  $q$  is the distributed transverse load.

The governing equations of equilibrium can be derived from Eqs. (17a)–(17c) by integrating the displacement gradients in mid-surface strains by parts and setting the coefficients of derivatives of mid-surface displacements to zero separately. Thus one obtains the following equilibrium equations for each displacement model.

For displacement model HOST12

$$\begin{aligned}
 \frac{\partial N_x}{\partial x} + \frac{\partial(N_{xy} + c_o M_{xy})}{\partial y} + \frac{Q_x}{R_x} &= 0, & \frac{\partial N_y}{\partial y} + \frac{\partial(N_{xy} - c_o M_{xy})}{\partial x} + \frac{Q_y}{R_y} &= 0, \\
 \frac{\partial Q_x}{\partial x} + \frac{\partial Q_y}{\partial y} - \frac{N_x}{R_x} - \frac{N_y}{R_y} + q &= 0, & \frac{\partial M_x}{\partial x} + \frac{\partial M_{xy}}{\partial y} - Q_x + \frac{S_x}{R_x} &= 0, \\
 \frac{\partial M_{xy}}{\partial x} + \frac{\partial M_y}{\partial y} - Q_y + \frac{S_y}{R_y} &= 0, & \frac{\partial S_x}{\partial x} + \frac{\partial S_y}{\partial y} - \frac{M_x}{R_x} - \frac{M_y}{R_y} - N_z &= 0, \\
 \frac{\partial N_x^*}{\partial x} + \frac{\partial(N_{xy}^* + c_o M_{xy}^*)}{\partial y} + \frac{Q_x^*}{R_x} - 2S_x &= 0, & \frac{\partial N_y^*}{\partial y} + \frac{\partial(N_{xy}^* - c_o M_{xy}^*)}{\partial x} + \frac{Q_y^*}{R_y} - 2S_y &= 0, \\
 \frac{\partial Q_x^*}{\partial x} + \frac{\partial Q_y^*}{\partial y} - \frac{N_x^*}{R_x} - \frac{N_y^*}{R_y} - 2M_z^* &= 0, & \frac{\partial M_x^*}{\partial x} + \frac{\partial M_{xy}^*}{\partial y} - 3Q_x^* + \frac{S_x^*}{R_x} &= 0, \\
 \frac{\partial M_{xy}^*}{\partial x} + \frac{\partial M_y^*}{\partial y} - 3Q_y^* + \frac{S_y^*}{R_y} &= 0, & \frac{\partial S_x^*}{\partial x} + \frac{\partial S_y^*}{\partial y} - \frac{M_x^*}{R_x} - \frac{M_y^*}{R_y} - 3N_z^* &= 0.
 \end{aligned} \tag{18}$$

In addition following line integrals are obtained

$$\begin{aligned}
 &\int_x (N_y \delta v_o + N_{xy} \delta u_o + N_y^* \delta v_o^* + N_{xy}^* \delta u_o^* + M_y \delta \theta_y + M_{xy} \delta \theta_x + C_o M_{xy} \delta u_o + M_y^* \delta \theta_y^* + M_{xy}^* \delta \theta_x^* + C_o M_{xy}^* \delta u_o^* + Q_y \delta w_o \\
 &+ Q_y^* \delta w_o^* + S_y \delta \theta_z + S_y^* \delta \theta_z^*) dx + \int_y (N_x \delta u_o + N_{xy} \delta v_o + N_x^* \delta u_o^* + N_{xy}^* \delta v_o^* + M_x \delta \theta_x + M_{xy} \delta \theta_y - C_o M_{xy} \delta v_o \\
 &+ M_x^* \delta \theta_x^* + M_{xy}^* \delta \theta_y^* - C_o M_{xy}^* \delta v_o^* + Q_x \delta w_o + Q_x^* \delta w_o^* + S_x \delta \theta_z + S_x^* \delta \theta_z^*) dy \\
 &= 0.
 \end{aligned} \tag{19}$$

The equilibrium equations for displacement models HOST11 and FOST are the first eleven and first five equations of displacement model HOST12 given in Eq. (18) respectively and the equations for displacement model HOST9 are same as the equations of displacement model HOST12 given in Eq. (18) by deleting the sixth, ninth and twelfth equations. Similarly in each displacement model the line integrals are also obtained.

### 6.1. Closed-form solutions

The exact form of the spatial variation of the solution of above equations can be obtained under the following boundary conditions:

Symmetric and antisymmetric cross-ply laminates.

Simply supported boundary conditions:

$$v_o = w_o = \theta_y = \theta_z = v_o^* = w_o^* = \theta_y^* = \theta_z^* = N_x = M_x = N_x^* = M_x^* = 0$$

on an edge  $x = \text{constant}$  and

$$u_o = w_o = \theta_x = \theta_z = u_o^* = w_o^* = \theta_x^* = \theta_z^* = N_y = M_y = N_y^* = M_y^* = 0$$

on an edge  $y = \text{constant}$ .

Sinusoidal variation of transverse load and temperature is considered as under:

$$\begin{aligned}
 q &= \sum_{m,n} q_{mn} \sin \alpha x \sin \beta y, & \alpha &= \frac{m\pi}{a}, & \beta &= \frac{n\pi}{b}, \\
 \Delta T &= \sum_{m,n} \left( T_{omn} + \frac{z}{h} T_{1mn} \right) \sin \alpha x \sin \beta y
 \end{aligned} \tag{20}$$

in which  $a$  and  $b$  are the dimensions of shell middle surface along the  $x$  and  $y$ -axes respectively and  $h$  is the thickness of shell.  $T_o$  is the average and  $T_1$  is the difference in rise in temperature of top and bottom surfaces of shell. The exact form of the spatial variation of mid-surface displacements is given by



$$\begin{aligned}
u_o &= \sum_{m,n}^{\infty} u_{omn} \cos \alpha x \sin \beta y, & v_o &= \sum_{m,n}^{\infty} v_{omn} \sin \alpha x \cos \beta y, \\
w_o &= \sum_{m,n}^{\infty} w_{omn} \sin \alpha x \sin \beta y, & \theta_x &= \sum_{m,n}^{\infty} \theta_{xmn} \cos \alpha x \sin \beta y, \\
\theta_y &= \sum_{m,n}^{\infty} \theta_{ymn} \sin \alpha x \cos \beta y, & \theta_z &= \sum_{m,n}^{\infty} \theta_{zmn} \sin \alpha x \sin \beta y, \\
u_o^* &= \sum_{m,n}^{\infty} u_{omn}^* \cos \alpha x \sin \beta y, & v_o^* &= \sum_{m,n}^{\infty} v_{omn}^* \sin \alpha x \cos \beta y, \\
w_o^* &= \sum_{m,n}^{\infty} w_{omn}^* \sin \alpha x \sin \beta y, & \theta_x^* &= \sum_{m,n}^{\infty} \theta_{xmn}^* \cos \alpha x \sin \beta y, \\
\theta_y^* &= \sum_{m,n}^{\infty} \theta_{ymn}^* \sin \alpha x \cos \beta y, & \theta_z^* &= \sum_{m,n}^{\infty} \theta_{zmn}^* \sin \alpha x \sin \beta y.
\end{aligned} \tag{21}$$

Clearly the assumed solution satisfies the boundary conditions stated above exactly. Substitution of Eq. (19) and series of Eq. (21) into Eq. (18) yields a set of linear algebraic equations in terms of the unknown amplitudes  $u_{omn}$ ,  $v_{omn}$ ,  $w_{omn}$ ,  $\theta_{xmn}$ ,  $\theta_{ymn}$ ,  $\theta_{zmn}$  and their higher-order (\*) terms. These equations can be expressed in matrix form as

$$\mathbf{C}' \Delta = \mathbf{F}. \tag{22}$$

Here  $\mathbf{C}'$ ,  $\Delta$  and  $\mathbf{F}$  for all the displacement models are given in Appendix C.

## 7. Discussion of numerical results

The primary purpose of the present paper is to highlight and compare the accuracy of the various higher-order theories in the light of available 3D solutions under mechanical loading and then to study the behaviour of composite and sandwich plates and shells under thermal loading.

**Example 1.** The examples presented by Bhimaraddi [24] are analysed here to compare the response of higher-order theories. Isotropic (Poisson's ratio = 0.3) and orthotropic spherical shells with following properties are analysed.

$$\begin{aligned}
\frac{E_x}{E_y} &= 25, & \frac{E_z}{E_y} &= 1, & \frac{G_{xz}}{E_y} &= \frac{G_{xy}}{E_y} = \frac{1}{2}, & \frac{G_{yz}}{E_y} &= \frac{1}{5}, \\
v_{xy} &= 0.25, & v_{zx} &= 0.03, & v_{yz} &= 0.4, & \text{hence } v_{xz} &= 0.75.
\end{aligned}$$

The centre deflection ( $wE_y/q$  at middle surface of the shell,  $x = a/2$ ,  $y = b/2$ ,  $z = 0$ ) values for homogeneous isotropic, orthotropic, antisymmetric cross-ply ( $0^\circ/90^\circ$ ) and symmetric cross-ply ( $0^\circ/90^\circ/0^\circ$ ) spherical shells (equal thickness in each layer) with different  $h/a$  and  $R/a$  ratios are shown in Tables 1–4 respectively. The results presented by all the theories are approximately same with thickness ratio  $h/a$  as 0.01, even with  $R/a$  ratio as 1 the difference with 3D is not more than 1.3%. But with thickness ratios higher than 0.1 and small curvature i.e.  $R/a$  less than 3 the error in all the theories comparing to 3D solutions presented by Bhimaraddi [24] is considerable. It is as high as 27.7% in the results of FOST and 21.9% in the results of HOST12 in case of symmetric cross-ply spherical shells with thickness ratio 0.15 and  $R/a$  ratio 1. One graph showing the non-dimensional centre deflection versus radius to side ( $R/a$ ) ratios in case of symmetric cross-ply ( $0^\circ/90^\circ/0^\circ$ ) spherical shell is shown in Fig. 2(a) and the percent error in non-dimensional centre deflection values is shown in Fig. 2(b) for 0.1 thickness ratio ( $h/a$ ). The error in all the higher-order theories is reduced with increase in values of  $R/a$  ratios. It is less than 6.3% with  $R/a$  ratios higher than 5 in HOST12 and HOST11 and less than 8% in HOST9 but in FOST the error is even upto 13% with thickness ratio ( $h/a$ ) as 0.1 and 16% with thickness ratios 0.15. The error in higher-order theories is less in other cases of laminate orientations and in descending order of error values are antisymmetric cross-ply, orthotropic and isotropic spherical shells respectively. In these cases the error is less than 5% even with  $R/a$  ratio 3 in all the theories. Thus the higher-order theories presented here are certainly an improvement over first-order theory and are in good agreement with 3D solutions in the range of even higher  $h/a$  ratios but with  $R/a$  ratio more than 3.

Table 1

Comparison of centre deflection ( $wE_y/q$ ) for isotropic ( $\nu = 0.3$ ) spherical shell with different  $h/a$  and  $R/a$  ratios ( $a/b = 1$ ,  $R_1 = R_2 = R$ )

$R/a$	$h/a$	HOST12	HOST11	HOST9	FOST	Bhimaraddi [24]
1	0.01	99.710	99.710	99.690	99.690	100.59
	0.1	7.8440	7.8440	7.7300	7.2300	8.7095
	0.15	4.2300	4.2300	4.1100	4.1100	4.9497
2	0.01	394.64	394.64	394.56	394.56	396.45
	0.1	17.530	17.530	17.340	17.340	18.451
	0.15	7.2250	7.2240	7.1000	7.1000	7.7240
3	0.01	872.59	872.59	872.41	872.41	875.36
	0.1	22.708	22.707	22.526	22.527	23.381
	0.15	8.3076	8.3072	8.1990	8.2800	8.5912
4	0.01	1514.6	1514.6	1514.3	1514.3	1518.3
	0.1	25.324	25.323	25.159	25.159	25.785
	0.15	8.7666	8.7664	8.6680	8.6690	8.9235
5	0.01	2296.8	2296.8	2296.3	2296.3	2301.4
	0.1	26.749	26.749	26.597	26.598	27.061
	0.15	8.9966	8.9964	8.9039	8.9052	9.0755
10	0.01	7375.1	7375.1	7373.9	7373.9	7383.1
	0.1	28.921	28.921	28.790	28.790	28.910
	0.15	9.3225	9.3225	9.2389	9.2404	9.2505
20	0.01	16490	16490	16488	16488	16499
	0.1	29.520	29.520	29.398	29.399	29.356
	0.15	9.4077	9.4077	9.3266	9.3282	9.2666
$\infty$ (plate)	0.01	28043	28043	28042	28042	29504
	0.1	29.725	29.725	29.606	29.607	29.44
	0.15	9.4365	9.4365	9.3560	9.3578	9.2352

Table 2

Comparison of centre deflection ( $wE_y/q$ ) for homogeneous orthotropic spherical shell with different  $h/a$  and  $R/a$  ratios ( $a/b = 1$ ,  $R_1 = R_2 = R$ )

$R/a$	$h/a$	HOST12	HOST11	HOST9	FOST	Bhimaraddi [24]
1	0.01	74.504	74.504	74.436	74.434	75.397
	0.1	3.9830	3.9780	3.8240	3.8240	4.7117
	0.15	2.0624	2.0584	1.9490	1.9540	2.5641
2	0.01	283.45	283.45	283.18	283.17	285.72
	0.1	5.5745	5.5720	5.4698	5.4760	5.9693
	0.15	2.4783	2.4765	2.4166	2.4289	2.6788
3	0.01	589.59	589.59	589.06	589.04	593.43
	0.1	6.0071	6.0057	5.9372	5.9461	6.2215
	0.15	2.5681	2.5672	2.5262	2.5406	2.6635
4	0.01	947.87	947.87	947.09	947.06	953.25
	0.1	6.1738	6.1730	6.1198	6.1298	6.3014
	0.15	2.6007	2.6001	2.5668	2.5820	2.6494
5	0.01	1318.8	1318.8	1317.8	1317.8	1325.5
	0.1	6.2540	6.2534	6.2080	6.2187	6.3332
	0.15	2.6159	2.6156	2.5860	2.6016	2.6393
10	0.01	2757.7	2757.7	2756.5	2756.5	2767.7
	0.1	6.3639	6.3638	6.3297	6.3411	6.3593
	0.15	2.6364	2.6363	2.6120	2.6281	2.6256
20	0.01	3791.9	3791.9	3791.3	3791.2	3802.5
	0.1	6.3920	6.3919	6.3610	6.3725	6.3532
	0.15	2.6416	2.6416	2.6185	2.6348	2.6022
$\infty$ (plate)	0.01	4333.7	4333.7	4333.5	4333.5	4343.0
	0.1	6.4014	6.4014	6.3713	6.3830	6.3343
	0.15	2.6433	2.6433	2.6210	2.6370	2.5879

Table 3

Comparison of centre deflection ( $wE_y/q$ ) for antisymmetric cross-ply (0/90) spherical shell with different  $h/a$  and  $R/a$  ratios ( $a/b = 1, R_1 = R_2 = R$ )

$R/a$	$h/a$	HOST12	HOST11	HOST9	FOST	Bhimaraddi [24]
1	0.01	53.564	53.564	53.557	53.553	54.129
	0.1	4.0666	4.0662	4.0226	4.0111	4.6920
	0.15	2.2155	2.2149	2.1694	2.1688	2.7386
2	0.01	211.07	211.07	211.05	211.09	212.33
	0.1	8.1661	8.1656	8.1097	8.1428	8.8092
	0.15	3.4615	3.4610	3.4153	3.4611	3.8190
3	0.01	463.40	463.40	463.40	463.36	456.46
	0.1	10.026	10.026	9.9787	10.053	10.512
	0.15	3.8573	3.8571	3.8174	3.8865	4.0856
4	0.01	796.77	796.77	796.86	796.79	799.81
	0.1	10.893	10.893	10.853	10.951	11.263
	0.15	4.0176	4.0175	3.9811	4.0610	4.1758
5	0.01	1194.5	1194.5	1194.8	1194.7	1198.7
	0.1	11.347	11.347	11.312	11.424	11.639
	0.15	4.0963	4.0962	4.0617	4.1470	4.2131
10	0.01	3572.2	3572.2	3575.9	3575.8	3584.8
	0.1	12.015	12.015	11.987	12.121	12.150
	0.15	4.2061	4.2061	4.1742	4.2676	4.2457
20	0.01	7110.6	7110.6	7126.4	7126.8	7142.6
	0.1	12.194	12.194	12.169	12.309	12.258
	0.15	4.2344	4.2344	4.2033	4.2988	4.2399
$\infty$ (plate)	0.01	10615	10615	10652	10653	10674
	0.1	12.255	12.255	12.231	12.373	12.257
	0.15	4.2439	4.2439	4.2131	4.3093	4.1291

Table 4

Comparison of centre deflection ( $wE_y/q$ ) for symmetric cross-ply (0/90/0) spherical shell with different  $h/a$  and  $R/a$  ratios ( $a/b = 1, R_1 = R_2 = R$ )

$R/a$	$h/a$	HOST12	HOST11	HOST9	FOST	Bhimaraddi [24]
1	0.01	53.626	53.624	53.613	53.609	54.252
	0.1	3.4132	3.4101	3.3583	3.2567	4.0811
	0.15	1.9004	1.8977	1.8536	1.7606	2.4345
2	0.01	208.86	208.86	206.81	206.78	208.36
	0.1	5.6510	5.6485	5.5955	5.3030	6.3134
	0.15	2.6871	2.6855	2.6483	2.4519	3.0931
3	0.01	439.30	439.28	439.19	439.10	441.81
	0.1	6.4220	6.4205	6.3763	5.9954	6.9888
	0.15	2.9050	2.9042	2.8135	2.6414	3.2228
4	0.01	724.02	724.00	723.85	723.65	727.62
	0.1	6.7432	6.7423	6.7032	6.2820	7.1476
	0.15	2.9895	2.9890	2.9614	2.7147	3.2605
5	0.01	1034.3	1034.2	1034.1	1033.7	1039.0
	0.1	6.9029	6.9023	6.8660	6.4241	7.3674
	0.15	3.0302	3.0300	3.0039	2.7499	3.2736
10	0.01	2413.1	2413.1	2412.7	2410.9	2422.4
	0.1	7.1278	7.1276	7.0957	6.6237	7.5127
	0.15	3.0862	3.0861	3.0624	2.7983	3.2769
20	0.01	3619.3	3619.3	3619.0	3615.0	3632.2
	0.1	7.1863	7.1862	7.1555	6.6756	7.5328
	0.15	3.1005	3.1005	3.0077	2.8107	3.2669
$\infty$ (plate)	0.01	4343.0	4343.0	4342.7	4342.7	4356.9
	0.1	7.2060	7.2060	7.1757	6.6930	7.5169
	0.15	3.1053	3.1053	3.0824	2.8148	3.2525

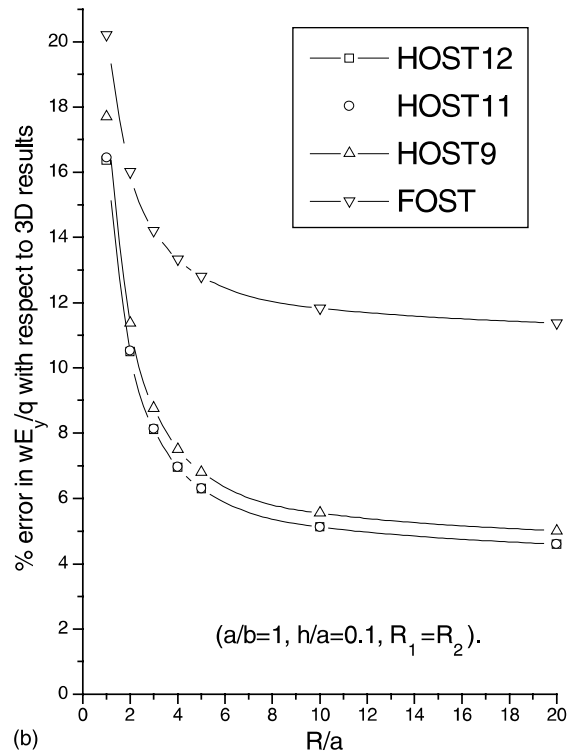
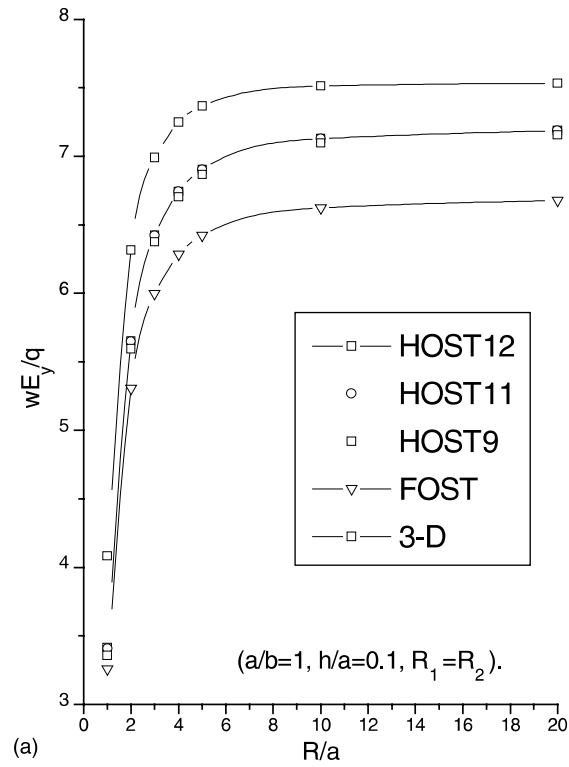


Fig. 2. (a) Non-dimensional centre deflection versus  $R/a$  ratio of simply supported symmetric cross-ply spherical shell subjected to sinusoidal load and (b) % error in (a).

**Example 2.** The exact solutions presented by Pagano [25] and Reddy [26] are illustrated in this example to compare the response of higher-order theories in the sandwich plates and shells. A square plate with various  $h/a$  ratios and a cylindrical shell with various  $h/a$  and  $R/a$  ratios are analysed here with following properties.

Face sheets :  $E_x = 25 \times 10^6$  psi,  $E_y = E_z = 1 \times 10^6$  psi,  $G_{xy} = 0.5 \times 10^6$  psi,  
 $G_{yz} = 0.2 \times 10^6$ ,  $G_{xz} = G_{xy}$ ,  $\nu_{xy} = \nu_{yz} = \nu_{xz} = 0.25$ ,  $h_f = 0.1h$ .  
 Core :  $E_x = E_y = 0.04 \times 10^6$  psi,  $E_z = 0.5 \times 10^6$  psi,  $G_{xy} = 0.016 \times 10^6$  psi,  
 $G_{xz} = G_{yz} = 0.06 \times 10^6$  psi,  $\nu_{zx} = \nu_{zy} = \nu_{xy} = 0.25$ ,  $h_c = 0.8h$ .  
 Hence  $\nu_{xy} = \nu_{yz} = 0.02$ .

Table 5 shows the values of non-dimensional centre deflection ( $100wE_y h^3 / qa^4$ ) in square orthotropic sandwich plate with different thickness ratios ( $h/a$ ). In the thin regime the results by all the theories are close to each other and in good agreement with 3D exact results presented by Pagano [25]. The error in the results presented by FOST is upto 29% and 37% in moderately thick and thick plates respectively comparing to 3D results. This error in the results presented by higher-order shear theories is only upto 5.5% even in thick regime. Table 6 shows the values of non-dimensional centre deflection ( $100wE_y h^3 / qa^4$ ) in orthotropic sandwich cylindrical shell with different thickness ratios ( $h/a$ ). The 3D and finite element solutions of this problem are presented by Reddy [26] and Menon [27] respectively. Again in the thin regime the results by all the theories are close to each other and comparable to 3D results. In thick shells error in FOST results is very high (30%) at  $h/a = 0.1$  and even more (upto 39%) at  $h/a = 0/25$ . The error in the results of higher-order shear deformation theories is 5–8% at  $h/a = 0.1$  and 6–10% at  $h/a = 0.25$  except in case of very low  $R/h$  ratio (i.e.  $R/h = 2$ ), as this ratio does not come under the perview of assumptions of present theories. The results of present formulation are maching well with the finite element results of thin shell higher-order theories presented by Menon [27].

**Example 3.** The 2D analytical solutions presented by Khdeir et al. [3] are compared and presented in this example to study the thermal effects on the response of cross-ply laminated shallow shells with variation of geometry and lamination. The non-dimensionalized centre deflection of cross-ply cylindrical ( $0^\circ/90^\circ$ ), spherical ( $0^\circ/90^\circ$ ) and ten layer cylindrical ( $0^\circ/90^\circ/\dots$ ) panels subjected to antisymmetric variation of temperature through thickness and uniform variation over the surface of the shell are presented in this example. The material and thickness of all the laminae are same with following properties:

Table 5  
 Comparison of centre deflection ( $100wE_y h^3 / qa^4$ ) for orthotropic sandwich plate with different  $h/a$  ratios ( $a/b = 1$ )

$h/a$	HOST12	HOST11	HOST9	FOST	Pagano [25]	Reddy [26]
0.01	0.88818	0.88818	0.89103	0.88522	0.892	0.8924
0.1	2.0823	2.0823	2.0848	1.5604	2.20	2.20046
0.25	7.1794	7.1794	7.1538	4.7666	7.596	7.5965

Table 6  
 Comparison of centre deflection ( $100wE_y h^3 / qa^4$ ) for orthotropic sandwich cylindrical shell with different  $h/a$  and  $R/h$  ratios ( $a/b = 1$ ,  $R_1 = R$ ,  $R_2 = \infty$ )

$h/a$	$R/h$	HOST12	HOST11	HOST9	FOST	Reddy [26]	Menon [27]	
							Theory 1	Theory 2
0.01	100	0.11774	0.11697	0.11800	0.11790	0.11863	–	–
	50	0.03255	0.03231	0.03262	0.03262	0.03294	–	–
	20	0.00521	0.00517	0.00523	0.00523	0.00535	–	–
0.1	100	2.0830	2.0830	2.0853	1.5615	2.2108	2.075	2.085
	50	2.0850	2.0850	2.0867	1.5646	2.2218	2.076	2.096
	20	2.0981	2.0981	2.0958	1.5858	2.2574	–	–
	10	2.1296	2.1294	2.1149	1.6551	2.3115	2.096	2.203
	5	2.0141	2.0117	1.9839	1.7734	2.1858	1.944	2.134
	2	0.3666	0.3581	0.3546	0.3135	0.4498	0.361	0.439
0.25	100	7.1803	7.1803	7.1547	4.7675	7.6310	–	–
	50	7.1831	7.1831	7.1571	4.7701	7.6669	–	–
	20	7.2024	7.2024	7.1741	4.7882	7.7816	–	–
	10	7.2710	7.2710	7.2344	4.8534	7.9959	–	–
	5	7.5377	7.5377	7.4680	5.1192	8.5081	–	–
	2	8.6990	8.6936	8.4688	6.9533	10.039	–	–

$$\frac{E_x}{E_y} = 25, \quad \frac{E_z}{E_y} = 1, \quad \frac{G_{xz}}{E_y} = \frac{G_{xy}}{E_y} = \frac{1}{2}, \quad \frac{G_{yz}}{E_y} = \frac{1}{5},$$

$$v_{xy} = v_{yz} = v_{xz} = 0.25, \quad \alpha_2/\alpha_1 = 3.$$

The non-dimensionalised deflection parameter

$$\bar{w} = \frac{w(a/2, b/2, 0)}{\alpha_1 T_1 b^2}$$

is used in the results. Mechanical loading and average temperature are zero. The results presented by all the theories are in good agreement with the corresponding theories presented by Khdeir et al. [3] as shown in Table 7.

**Example 4.** A new problem is chosen here to study the thermal effects on the response of sandwich shells with variation of geometry and lamination in orthotropic and cross-ply cylindrical and spherical panels under a temperature variation, uniform over the surface and antisymmetric through the thickness of the shell. The geometric and material properties are same as used in Example 2 with assuming the linear coefficients of thermal expansion as under:

$$\text{Face sheets : } \alpha_1 = 0.1 \times 10^{-5}/^\circ\text{C}, \quad \alpha_2 = 2 \times 10^{-5}/^\circ\text{C}, \quad \alpha_3 = \alpha_1.$$

$$\text{Core : } \alpha_1 = 0.1 \times 10^{-6}/^\circ\text{C}, \quad \alpha_2 = 0.2 \times 10^{-5}/^\circ\text{C}, \quad \alpha_3 = \alpha_1.$$

Table 8 shows the non-dimensionalized centre deflections  $\bar{w} = 10wh/(a^2\alpha_1 T_1)$  in orthotropic sandwich cylindrical and spherical shells subjected to sinusoidal temperature load with different  $R/a$  and  $h/a$  ratios for all the theories used here. The uniformly distributed load ( $q$ ) and average temperature  $T_o$  are considered to be zero here. In the thin regime, i.e.  $h/a = 0.01$ , the results presented by all the theories are matching well with each other. The maximum difference in the results of first-order shear theory (FOST) and the results of the displacement model HOST12 of higher-order shear theories is 2% in thin regime. Further with increase of  $h/a$  ratios the difference in the results of first- and higher-order shear theories increases enormously and is 14% in case of  $h/a = 0.1$  and 23% in case of  $h/a = 0.25$ . The results in these two cases are plotted in Fig. 3(a) and Fig. 3(b) with respect to various  $R/a$  ratios. As is already seen in above examples the results of higher-order shear deformation theories are closer to the 3D exact solution, in this example these should be considered to be more reliable and may be used for further reference to numerical or analytical solutions of temperature loading.

Tables 9 and 10 show the non-dimensionalized centre deflection defined earlier in antisymmetric ( $0^\circ/\text{core}/90^\circ$ ), and symmetric ( $0^\circ/90^\circ/\text{core}/90^\circ/0^\circ$ ) cross-ply sandwich cylindrical and spherical shells respectively subjected to sinusoidal temperature load. The results presented by all the theories are not deviating much particularly in the thick regime in these two cases. The maximum difference is 2% in thick and 3% in thin regime.

Table 7

Non-dimensionalized centre deflections  $\bar{w}$  of cross-ply shells subjected to sinusoidal temperature load with different  $R/a$  ratios

$R/a$	HOST12	HOST11	HOST9	FOST	Khdeir [3]		
					HSDT	FSDT	CST
<i>Cylindrical shell (0/90) with <math>a/b = 1, h/a = 0.1, R_1 = \infty, R_2 = R</math></i>							
5	1.1261	1.1261	1.1279	1.1272	1.1235	1.1248	1.1280
10	1.1434	1.1434	1.1449	1.1444	1.1421	1.1439	1.1447
50	1.1493	1.1493	1.1507	1.1501	1.1482	1.1501	1.1501
<i>Spherical shell (0/90) with <math>a/b = 1, h/a = 0.1, R_1 = R_2 = R</math></i>							
5	1.0588	1.0588	1.0602	1.0578	1.0545	1.0546	1.0660
10	1.1256	1.1256	1.1269	1.1258	1.1235	1.1248	1.1280
50	1.1487	1.1487	1.1500	1.1493	1.1475	1.1493	1.1494
Plate	1.1497	1.1497	1.1510	1.1504	1.1485	1.1504	1.1504
<i>Ten layer cylindrical shell (0/90/... ) with <math>a/b = 1, h/a = 0.1, R_1 = \infty, R_2 = R</math></i>							
5	1.0224	1.0224	1.0239	1.0234	1.0216	1.0215	1.0247
10	1.0299	1.0299	1.0312	1.0307	1.0303	1.0302	1.0310
50	1.0325	1.0325	1.0337	1.0330	1.0332	1.0330	1.0331
Plate	1.0326	1.0326	1.0339	1.0331	1.0333	1.0331	1.0331

Table 8

Non-dimensionalized centre deflections  $\bar{w}$  of orthotropic sandwich shells subjected to sinusoidal temperature load with different  $R/a$  and  $h/a$  ratios

$R/a$	$h/a$	HOST12	HOST11	HOST9	FOST
<i>Cylindrical shell with <math>a/b = 1, R_1 = \infty, R_2 = R</math></i>					
5	0.01	1.43467	1.43231	1.40776	1.40652
	0.1	2.49668	2.49650	2.46217	2.14244
	0.25	4.22802	4.22787	4.21900	3.26804
10	0.01	1.70695	1.60612	1.67497	1.67189
	0.1	2.51013	2.51009	2.47518	2.15131
	0.25	4.24059	4.24055	4.23050	3.27583
20	0.01	1.79187	1.79164	1.75833	1.75457
	0.1	2.51351	2.51350	2.47845	2.15354
	0.25	4.24374	4.24373	4.23337	3.27778
<i>Spherical shell with <math>a/b = 1, R_1 = R_2 = R</math></i>					
5	0.01	0.877956	0.874442	0.861476	0.862432
	0.1	2.46373	2.46345	2.42979	2.12390
	0.25	4.20316	4.20297	4.19525	3.26282
10	0.01	1.43679	1.43447	1.40977	1.40854
	0.1	2.50176	2.50169	2.46695	2.14663
	0.25	4.23434	4.23429	4.22452	3.27453
20	0.01	1.70767	1.70685	1.67565	1.67258
	0.1	2.51141	2.51139	2.42639	2.15236
	0.25	4.24217	4.24216	4.23188	3.27746
Plate	0.01	1.82208	1.82208	1.78798	1.78397
	0.1	2.51464	2.51464	2.47955	2.15428
	0.25	4.24478	4.24478	4.23433	3.27843

**Example 5.** To compare the stresses computed by the present formulation under mechanical and thermal loading following two cases are considered with the same material properties as used in Example 2.

(a) An analysis of a layered laminated ( $0^\circ/90^\circ/0^\circ$ ) circular cylindrical shell roof with simply supported edges is carried out and the results are compared with available elasticity solution given by Ren [28] under mechanical loading. The shell roof has a radius  $R = 5$  units, length  $b = 30$  units and subtended angle of 60 degrees. A sinusoidal load  $q = q_o \sin(\pi x/a) \sin(\pi y/b)$  is applied on the shell surface. The thickness of each layer is  $h/4, h/2$  and  $h/4$  respectively as per their orientation. Numerical results are obtained for different  $R/h$  ratios, namely 100, 10, 5, and 2 and are presented in Table 11. The maximum deflection and the normal stresses at the centre  $(a/2, b/2)$  and the shear stress at the support  $(0, 0)$  are normalized as

$$\bar{w} = 100wE_y/(q_o h s^4), \quad (\bar{\sigma}_x, \bar{\sigma}_y, \bar{\tau}_{xy}) = (\sigma_x, \sigma_y, \tau_{xy})/(q_o s^2), \quad s = R/h.$$

The percentage difference between the present and the elasticity solutions is presented in the bracket below each value. It is observed from these results that for lower  $R/h$  ratios, both stress and displacement fields, given by the higher-order shear deformation theories are close to the exact three-dimensional solutions while comparing with the results of first-order shear theory.

(b) The thermal bending of simply supported, symmetric ( $0^\circ/90^\circ/0^\circ$ ) and antisymmetric ( $0^\circ/90^\circ$ ) cross-ply square plates is considered in this example. The temperature rise is assumed to be sinusoidally distributed as

$$\Delta T = \left(T_o + \frac{z}{h} T_1\right) \sin(\pi x/a) \sin(\pi y/b) \text{ in which } T_o = 0 \text{ and } T_1 = 1.$$

The layers are of equal thickness. The results of this problem are compared with available analytical solution of discrete layer theory given by He [12]. Numerical results are obtained for two  $a/h$  ratios, namely 5 and 10 and are presented in Tables 12 and 13. The maximum deflection and the normal stresses at the centre  $(a/2, a/2)$  and the transverse shear stresses at the support  $[\tau_{xy}(0, 0), \tau_{xz}(0, a/2), \text{ and } \tau_{yz}(a/2, 0)]$  are normalized as

$$\bar{w} = 10hw/(\alpha_1 T_1 a^2), \quad (\bar{\sigma}_x, \bar{\sigma}_y, \bar{\tau}_{xy}, \bar{\tau}_{xz}, \bar{\tau}_{yz}) = (\sigma_x, \sigma_y, \tau_{xy}, \tau_{xz}, \tau_{yz})10h/(\alpha_1 T_1 E_y a).$$

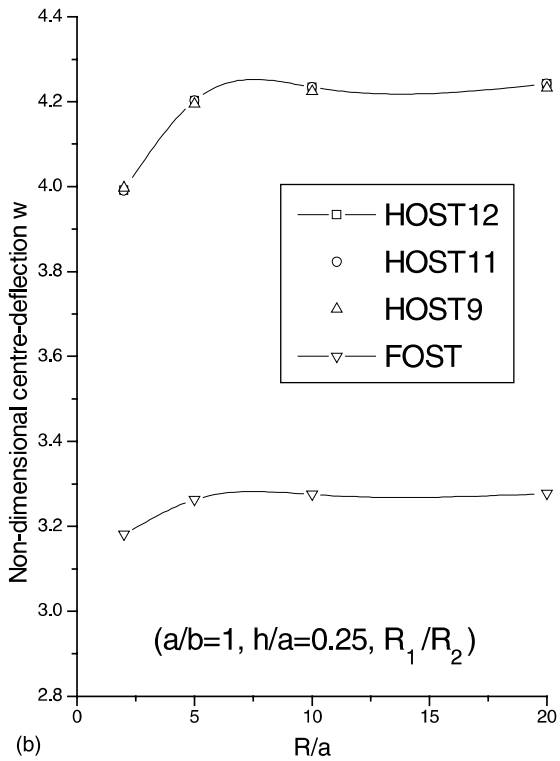
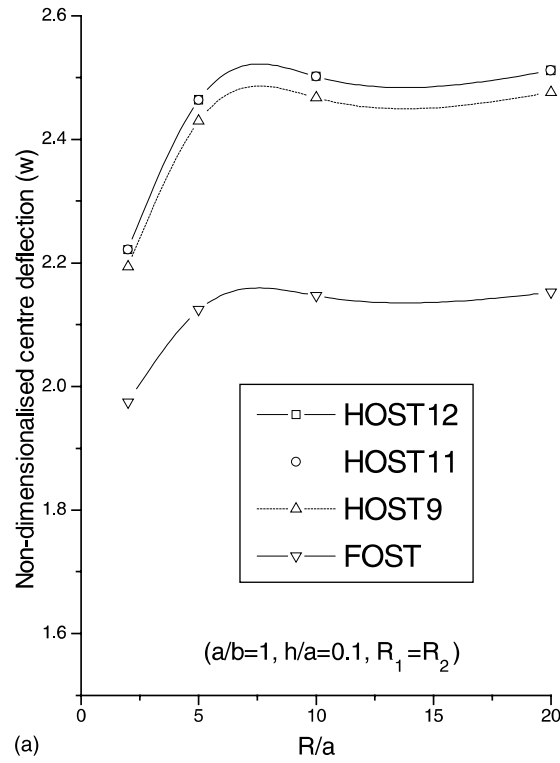


Fig. 3. (a,b) Non-dimensional centre deflection versus  $R/a$  ratio of simply supported orthotropic sandwich spherical shell subjected to sinusoidal temperature load.

It is observed that the results presented by the higher-order shear theories of present formulation are close to the results given by He [12] while the first-order shear theory under-predicts the results, in general.



Table 9

Non-dimensionalized centre deflections  $\bar{w}$  of antisymmetric cross-ply sandwich (0/core/90) shells subjected to sinusoidal temperature load with different  $R/a$  and  $h/a$  ratios

$R/a$	$h/a$	HOST12	HOST11	HOST9	FOST
<i>Cylindrical shell with <math>a/b = 1, R_1 = \infty, R_2 = R</math></i>					
5	0.01	2.56432	2.56368	2.47910	2.47964
	0.1	6.57874	6.57865	6.47152	6.47765
	0.25	6.64641	6.64635	6.57582	6.62009
10	0.01	4.75854	4.75799	4.64179	4.64214
	0.1	6.63063	6.63061	6.52688	6.53324
	0.25	6.60229	6.60227	6.53658	6.58232
20	0.01	6.05362	6.05340	5.93405	5.93417
	0.1	6.63772	6.63771	6.53587	6.54297
	0.25	6.57810	6.57810	6.51479	6.56187
<i>Spherical shell with <math>a/b = 1, R_1 = R_2 = R</math></i>					
5	0.01	0.885045	0.884719	0.862706	0.862964
	0.1	6.20150	6.20118	6.10588	6.12662
	0.25	6.45154	6.45132	6.39433	6.45714
10	0.01	2.53488	2.53425	2.47684	2.47738
	0.1	6.51914	6.51905	6.42031	6.43204
	0.25	6.52690	6.52684	6.46685	6.51931
20	0.01	4.73032	4.72977	4.63899	4.63950
	0.1	6.60338	6.60336	6.50379	6.51294
	0.25	6.54602	6.54600	6.48527	6.53504
Plate	0.01	6.64726	6.64726	6.54029	6.54037
	0.1	6.63198	6.63198	6.53213	6.54037
	0.25	6.55254	6.55254	6.49156	6.54037

Table 10

Non-dimensionalized centre deflections  $\bar{w}$  of symmetric cross-ply sandwich (0/90/core/90/0) shells subjected to sinusoidal temperature load with different  $R/a$  and  $h/a$  ratios

$R/a$	$h/a$	HOST12	HOST11	HOST9	FOST
<i>Cylindrical shell with <math>a/b = 1, R_1 = \infty, R_2 = R</math></i>					
5	0.01	1.32704	1.32690	1.30120	1.30218
	0.1	1.80304	1.80305	1.78069	1.77727
	0.25	1.79713	1.79713	1.83620	1.79004
10	0.01	1.66168	1.66163	1.63018	1.63053
	0.1	1.81008	1.81008	1.78755	1.78261
	0.25	1.79640	1.79640	1.85394	1.78983
20	0.01	1.77326	1.77325	1.73995	1.74003
	0.1	1.81184	1.81184	1.78927	1.78395
	0.25	1.79713	1.79713	1.83620	1.79004
<i>Spherical shell with <math>a/b = 1, R_1 = R_2 = R</math></i>					
5	0.01	0.733198	0.733022	0.718389	0.719637
	0.1	1.76909	1.76913	1.74783	1.74992
	0.25	1.77381	1.77393	1.81551	1.77707
10	0.01	1.32657	1.32643	1.30074	1.30175
	0.1	1.80144	1.80144	1.77918	1.77568
	0.25	1.79146	1.79149	1.83118	1.77685
20	0.01	1.66139	1.66134	1.62990	1.63026
	0.1	1.80967	1.80967	1.78717	1.78221
	0.25	1.79589	1.79590	1.83511	1.78930
Plate	0.01	1.81384	1.81384	1.77989	1.77985
	0.1	1.81242	1.81242	1.78984	1.78439
	0.25	1.79737	1.79737	1.83643	1.79011

Table 11

Maximum non-dimensionalized centre deflection ( $\bar{w}$ ) and stresses for a simply supported three-layered (0/90/0) laminated cylindrical shell roof for different  $R/h$  ratios

Quantity	$R/h$	HOST12	HOST11	HOST9	FOST	3D Ren [28]
$\bar{w}$	100	0.5421 (1.70)	0.5421 (1.70)	0.5417 (1.63)	0.5404 (1.39)	0.533
	10	1.4706 (-6.75)	1.4688 (-6.86)	1.4525 (-7.89)	1.3147 (-16.63)	1.577
	5	3.3070 (-10.48)	3.3020 (-10.61)	3.2396 (-12.30)	2.7547 (-25.43)	3.694
	2	14.460 (-13.56)	14.459 (-13.56)	14.022 (-16.18)	12.737 (-23.86)	16.728
$\bar{\sigma}_x(z = \pm h/2)$	100	0.5443 (2.12) -0.5358 (-2.23)	0.5439 (2.05) -0.5362 (-2.15)	0.5439 (2.05) -0.5360 (-2.19)	0.5422 (1.73) -0.5355 (-2.28)	0.533 -0.548
	10	0.9428 (-1.48) -0.9658 (-8.70)	0.9384 (-1.94) -0.9665 (-8.62)	0.9397 (-1.81) -0.9638 (-8.90)	0.8168 (-14.65) -0.862 (-18.52)	0.957 -1.058
	5	1.2312 (-1.66) -1.2916 (-17.31)	1.2280 (-1.92) -1.2888 (-17.49)	1.2368 (-1.21) -1.2744 (-18.41)	0.7944 (-36.55) -0.8872 (-43.20)	1.252 -1.562
	2	2.3480 (-10.96) -2.6425 (-33.12)	2.3458 (-11.04) -2.6375 (-33.24)	2.5175 (-4.50) -2.5150 (-36.34)	0.7143 (-72.91) -0.9483 (-76.00)	2.637 -3.951
$\bar{\sigma}_y(z = \pm h/2)$	100	0.01547 (-1.46) 0.00311 (-2.81)	0.01516 (-3.44) 0.00280 (-12.50)	0.01538 (-2.04) 0.00310 (-3.12)	0.01534 (-2.29) 0.00308 (-6.25)	0.0157 -0.0032
	10	0.01359 (-20.06) -0.00969 (-2.12)	0.01106 (-34.94) -0.01218 (23.03)	0.01387 (-18.41) -0.00907 (-8.38)	0.01219 (-28.29) -0.00811 (-18.08)	0.017 -0.0099
	5	0.0178 (-41.83) -0.0161 (-5.85)	0.01358 (-55.62) -0.0201 (17.50)	0.0195 (-36.27) -0.0140 (-18.13)	0.01386 (-39.22) -0.00994 (-41.87)	0.0306 -0.0171
	2	0.02543 (-77.6) -0.04160 (-14.93)	0.02376 (-79.10) -0.04320 (-11.66)	0.04575 (-59.70) -0.03410 (-30.26)	0.02435 (-78.55) -0.01725 (-64.72)	0.1135 -0.0489
$\bar{\tau}_{xy}(z = \pm h/2)$	100	-0.01697 (-2.47) 0.02485 (-1.78)	-0.01697 (-2.47) 0.02485 (-1.78)	-0.01709 (-1.80) 0.02474 (-2.21)	-0.01706 (-1.95) 0.02468 (-2.45)	-0.0174 0.0253
	10	-0.003617 (16.68) 0.01408 (-7.97)	-0.003605 (16.68) 0.01406 (-8.10)	-0.00291 (-6.13) 0.01391 (-9.10)	-0.002446 (-21.10) 0.01256 (-17.91)	-0.0031 0.0153
	5	-0.01098 (14.38) 0.0218 (-14.84)	-0.01096 (14.17) 0.021732 (-15.11)	-0.00937 (-2.39) 0.021096 (-17.59)	-0.006732 (-29.89) 0.017204 (-32.79)	-0.0096 0.0256

Table 11 (continued)

Quantity	R/h	HOST12	HOST11	HOST9	FOST	3D Ren [28]
	2	-0.0442 (26.28) 0.05863 (-21.83)	-0.04423 (26.37) 0.05855 (-21.93)	-0.03805 (8.71) 0.05373 (-28.36)	-0.02503 (-28.49) 0.04325 (-42.33)	-0.0350 0.0750

Table 12

Maximum non-dimensionalized centre deflection ( $\bar{w}$ ) and stresses in a simply supported symmetric cross-ply (0/90/0) square plate under thermal loading

a/h	Quantity	HOST12	HOST11	HOST9	FOST	He [12]
5	$\bar{w}$	1.0823	1.0823	1.0874	1.0763	1.0904
	$\bar{\sigma}_x^2(z = -h/6)$	0.6628	0.6628	0.6616	0.6556	0.6712
	$\bar{\sigma}_x^1(z = -h/6)$	0.3024	0.3024	0.2736	0.1357	0.4776
	$\bar{\sigma}_x^1(z = -h/2)$	0.01215	0.01215	0.08264	0.4072	0.1478
	$\bar{\sigma}_y^2(z = -h/6)$	-0.8550	-0.8550	-0.9838	-1.0208	-0.8265
	$\bar{\sigma}_y^1(z = -h/2)$	1.8538	1.8538	1.8590	1.8618	1.8450
	$\bar{\tau}_{xy}^1(z = -h/2)$	1.0814	1.0814	1.0786	1.0722	1.0850
	$\bar{\tau}_{xz}(z = -h/6)$	0.1263	0.1263	0.1272	0.07948	0.0844
	$\bar{\tau}_{xz}(z = 0)$	0.1433	0.1433	0.1448	0.07948	0.0674
	$\bar{\tau}_{yz}(z = -h/6)$	-0.1055	-0.1055	-0.1046	0.10598	-0.1094
	$\bar{\tau}_{yz}(z = 0)$	-0.04136	-0.04136	-0.04088	0.0424	-0.0480
10	$\bar{w}$	1.04889	1.04889	1.05013	1.04602	1.0517
	$\bar{\sigma}_x^2(z = -h/6)$	0.3308	0.3308	0.3306	0.3296	0.3325
	$\bar{\sigma}_x^1(z = -h/6)$	0.05808	0.05808	0.05395	0.02822	0.0960
	$\bar{\sigma}_x^1(z = -h/2)$	0.01647	0.01647	0.02656	0.08467	0.0361
	$\bar{\sigma}_y^2(z = -h/6)$	-0.1590	-0.1590	-0.1630	-0.1621	-0.1436
	$\bar{\sigma}_y^1(z = -h/2)$	0.9705	0.9705	0.9712	0.9715	0.9690
	$\bar{\tau}_{xy}^1(z = -h/2)$	0.5192	0.5192	0.5188	0.5178	0.5200
	$\bar{\tau}_{xz}(z = -h/6)$	0.04329	0.04329	0.4336	0.02616	0.0293
	$\bar{\tau}_{xz}(z = 0)$	0.04971	0.04971	0.04981	0.02616	0.0250
	$\bar{\tau}_{yz}(z = -h/6)$	-0.03553	-0.03553	0.03547	0.03488	-0.0316
	$\bar{\tau}_{yz}(z = 0)$	-0.01443	-0.01443	0.01440	0.01395	-0.0234

Table 13

Maximum non-dimensionalized centre deflection ( $\bar{w}$ ) and stresses in a simply supported antisymmetric cross-ply (0/90) square plate under thermal loading

a/h	Quantity	HOST12	HOST11	HOST9	FOST	He [12]
5	$\bar{w}$	1.1478	1.1478	1.15297	1.1504	1.1557
	$\bar{\sigma}_x^2(z = 0)$	0.06566	0.06566	0.06764	0.0700	0.0589
	$\bar{\sigma}_x^2(z = h/2)$	-1.7096	-1.7096	-1.7114	-1.7654	-1.6956
	$\bar{\sigma}_x^1(z = 0)$	2.2160	2.2160	2.2320	2.3100	1.9444
	$\bar{\sigma}_x^1(z = -h/2)$	-0.2410	-0.2410	-0.1818	-0.6148	-0.3077
	$\bar{\sigma}_y^2(z = 0)$	-2.2160	-2.2160	2.2320	-2.3100	-1.9444
	$\bar{\sigma}_y^2(z = h/2)$	0.2410	0.2410	0.1818	0.6148	0.3077
	$\bar{\tau}_{xy}^2(z = h/2)$	-1.1576	-1.1576	-1.1556	-1.1354	-1.1653
	$\bar{\tau}_{xz}(z = 0)$	-0.03646	-0.03646	-0.03544	-	-0.0740
	$\bar{\tau}_{yz}(z = 0)$	-0.03646	-0.03646	-0.03544	-	-0.0740
10	$\bar{w}$	1.1497	1.1497	1.1510	1.1504	1.1519
	$\bar{\sigma}_x^2(z = 0)$	0.03387	0.03387	0.03469	0.0350	0.0334
	$\bar{\sigma}_x^2(z = h/2)$	-0.8748	-0.8748	-0.8753	-0.8827	-0.8728
	$\bar{\sigma}_x^1(z = 0)$	1.1430	1.1430	1.1450	1.1550	1.1032
	$\bar{\sigma}_x^1(z = -h/2)$	-0.2547	-0.2547	-0.2460	-0.3074	-0.2638
	$\bar{\sigma}_y^2(z = 0)$	-1.1430	-1.1430	-1.1450	-1.1550	-1.1032
	$\bar{\sigma}_y^2(z = h/2)$	0.2547	0.2547	0.2460	0.3074	0.2638
	$\bar{\tau}_{xy}^2(z = h/2)$	-0.5707	-0.5707	-0.5704	-0.5677	-0.5719
	$\bar{\tau}_{xz}(z = 0)$	-0.01039	-0.01039	-0.01031	-	-0.0210
	$\bar{\tau}_{yz}(z = 0)$	-0.01039	-0.01039	-0.01031	-	-0.0210

## 8. Conclusions

Closed-form formulations of 2D higher-order shear deformation theory are presented for the analysis of simply supported composite and sandwich laminated doubly curved shells under thermo-mechanical loading conditions. These solutions are also applicable to the plates by taking both the radii of curvature as infinity and cylindrical shells by taking one radius of curvature as infinity. The present results are compared with the exact solutions available in the literature. The results presented by the higher-order theories are found closer to the exact results in comparison to the results obtained by first-order shear-deformation theory. Particularly in case of sandwich laminates, where the error in the results of first-order shear deformation theory with respect to the results of 3D is large (upto 40% even in deflection), the error in the results of higher-order shear deformation theories is not more than 5–10%. Thus, the importance of higher-order shear deformation theories especially for sandwich laminates is established beyond any doubt.

## Acknowledgements

First author is thankful to the Director, M.P. Council of Science and Technology, Bhopal, India and the Director, S.G.S. Institute of Technology and Science, Indore, India for allowing him to conduct this research at IIT Bombay under FTYS scheme of MPCOST.

## Appendix A

Reduced elastic constants of the orthotropic material corresponding to  $L$ th lamina:  
For displacement model HOST12 and HOST11

$$\begin{aligned} Q_{22} &= C_{11}s^4 + 2(C_{12} + 2C_{44})s^2c^2 + C_{22}c^4, \\ Q_{23} &= C_{13}s^2 + C_{23}c^2, \\ Q_{24} &= (C_{11} - C_{12} - 2C_{44})s^3c + (C_{12} - C_{22} + 2C_{44})c^3s, \\ Q_{33} &= C_{33}, \\ Q_{34} &= (C_{31} - C_{32})sc, \\ Q_{44} &= (C_{11} - 2C_{12} + C_{22} - 2C_{44})s^2c^2 + C_{44}(c^4 + s^4), \\ Q_{55} &= C_{55}c^2 + C_{66}s^2, \\ Q_{56} &= (C_{55} - C_{66})sc, \\ Q_{66} &= C_{55}s^2 + C_{66}c^2 \quad \text{and} \quad Q_{ij} = Q_{ji}, \quad i, j = 1, 6. \end{aligned}$$

For displacement model HOST9 and FOST

$$\begin{aligned} \bar{Q}_{11} &= \bar{C}_{11}c^4 + 2(\bar{C}_{12} + 2\bar{C}_{33})s^2c^2 + \bar{C}_{22}s^4, \\ \bar{Q}_{12} &= \bar{C}_{12}(c^4 + s^4) + (\bar{C}_{11} + \bar{C}_{22} - 4\bar{C}_{33})s^2c^2, \\ \bar{Q}_{13} &= (\bar{C}_{11} - \bar{C}_{12} - 2\bar{C}_{33})sc^3 + (\bar{C}_{12} - \bar{C}_{22} + 2\bar{C}_{33})c^3s, \\ \bar{Q}_{22} &= \bar{C}_{11}s^4 + 2(\bar{C}_{12} + 2\bar{C}_{33})s^2c^2 + \bar{C}_{22}c^4, \\ \bar{Q}_{23} &= (\bar{C}_{11} - \bar{C}_{12} - 2\bar{C}_{33})s^3c + (\bar{C}_{12} - \bar{C}_{22} + 2\bar{C}_{33})c^3s, \\ \bar{Q}_{33} &= (\bar{C}_{11} - 2\bar{C}_{12} + \bar{C}_{22} - 2\bar{C}_{33})s^2c^2 + C_{33}(c^4 + s^4), \\ \bar{Q}_{44} &= \bar{C}_{44}c^2 + \bar{C}_{55}s^2, \\ \bar{Q}_{45} &= (\bar{C}_{44} - \bar{C}_{55})sc, \\ \bar{Q}_{55} &= \bar{C}_{44}s^2 + \bar{C}_{55}c^2 \quad \text{and} \quad \bar{Q}_{ij} = \bar{Q}_{ji}, \quad i, j = 1 \text{ to } 5 \end{aligned}$$

in which  $s = \sin \theta$  and  $c = \cos \theta$ .

**Appendix B**

Membrane, flexure, coupling and shear rigidity matrices for various models:

For displacement model HOST12 and HOST11

$$\mathbf{D}_m = \sum_{L=1}^{NL} \begin{bmatrix} Q_{11}H_1 & Q_{12}H_1 & Q_{14}H_1 & Q_{11}H_3 & Q_{12}H_3 & Q_{14}H_3 & Q_{13}H_1 & Q_{13}H_3 \\ & Q_{22}H_1 & Q_{24}H_1 & Q_{12}H_3 & Q_{22}H_3 & Q_{24}H_3 & Q_{23}H_1 & Q_{23}H_3 \\ & & Q_{44}H_1 & Q_{14}H_3 & Q_{24}H_3 & Q_{44}H_3 & Q_{34}H_1 & Q_{34}H_3 \\ & & & Q_{11}H_5 & Q_{12}H_5 & Q_{14}H_5 & Q_{13}H_3 & Q_{13}H_5 \\ & & & & Q_{22}H_5 & Q_{24}H_5 & Q_{23}H_3 & Q_{23}H_5 \\ & & & & & Q_{44}H_5 & Q_{34}H_3 & Q_{34}H_5 \\ & & & & & & Q_{33}H_1 & Q_{33}H_3 \\ & & & & & & & Q_{33}H_3 \end{bmatrix},$$

Symmetric

$$\mathbf{D}_b = \sum_{L=1}^{NL} \begin{bmatrix} Q_{11}H_3 & Q_{12}H_3 & Q_{14}H_3 & Q_{11}H_5 & Q_{12}H_5 & Q_{14}H_5 & Q_{13}H_3 \\ & Q_{22}H_3 & Q_{24}H_3 & Q_{12}H_5 & Q_{22}H_5 & Q_{24}H_5 & Q_{23}H_3 \\ & & Q_{44}H_3 & Q_{14}H_5 & Q_{24}H_5 & Q_{44}H_5 & Q_{34}H_3 \\ & & & Q_{11}H_7 & Q_{12}H_7 & Q_{14}H_7 & Q_{13}H_5 \\ & & & & Q_{22}H_7 & Q_{24}H_7 & Q_{23}H_5 \\ & & & & & Q_{44}H_7 & Q_{34}H_5 \\ & & & & & & Q_{33}H_3 \end{bmatrix},$$

Symmetric

$$\mathbf{D}_c = \sum_{L=1}^{NL} \begin{bmatrix} Q_{11}H_2 & Q_{12}H_2 & Q_{14}H_2 & Q_{11}H_4 & Q_{12}H_4 & Q_{14}H_4 & Q_{13}H_2 \\ & Q_{22}H_2 & Q_{24}H_2 & Q_{12}H_4 & Q_{22}H_4 & Q_{24}H_4 & Q_{23}H_2 \\ & & Q_{44}H_2 & Q_{14}H_4 & Q_{24}H_4 & Q_{44}H_4 & Q_{34}H_2 \\ & & & Q_{11}H_4 & Q_{12}H_6 & Q_{14}H_6 & Q_{13}H_4 \\ & & & & Q_{22}H_6 & Q_{24}H_6 & Q_{23}H_4 \\ & & & & & Q_{44}H_6 & Q_{34}H_4 \\ & & & & & & Q_{33}H_2 \\ Q_{13}H_4 & Q_{23}H_4 & Q_{34}H_4 & Q_{13}H_6 & Q_{23}H_6 & Q_{34}H_6 & Q_{33}H_4 \end{bmatrix},$$

Symmetric

$$\mathbf{D}_s = \sum_{L=1}^{NL} \begin{bmatrix} Q_{55}H_1 & Q_{56}H_1 & Q_{55}H_3 & Q_{56}H_3 & Q_{55}H_2 & Q_{56}H_2 & Q_{55}H_4 & Q_{56}H_4 \\ & Q_{66}H_1 & Q_{56}H_3 & Q_{66}H_3 & Q_{56}H_2 & Q_{66}H_2 & Q_{56}H_4 & Q_{66}H_4 \\ & & Q_{55}H_5 & Q_{56}H_5 & Q_{55}H_4 & Q_{56}H_4 & Q_{55}H_6 & Q_{56}H_6 \\ & & & Q_{66}H_5 & Q_{56}H_4 & Q_{66}H_4 & Q_{56}H_6 & Q_{66}H_6 \\ & & & & Q_{55}H_3 & Q_{56}H_3 & Q_{55}H_5 & Q_{56}H_5 \\ & & & & & Q_{66}H_3 & Q_{56}H_5 & Q_{66}H_5 \\ & & & & & & Q_{55}H_7 & Q_{56}H_7 \\ & & & & & & & Q_{66}H_7 \end{bmatrix},$$

Symmetric

$$H_i = \frac{(z_{L+1}^i - z_L^i)}{i}, \quad i = 1, 2, \dots, 7.$$

For displacement model HOST9

The elements of the  $\mathbf{D}_m$ ,  $\mathbf{D}_c$  and  $\mathbf{D}_b$  matrices are same as given for displacement models HOST12 and HOST11 and the elements of  $\mathbf{D}_s$  matrix are given below:

$$\mathbf{D}_s = \sum_{L=1}^{NL} \begin{bmatrix} \bar{Q}_{44}H_1 & \bar{Q}_{45}H_1 & \bar{Q}_{44}H_3 & \bar{Q}_{45}H_3 & \bar{Q}_{44}H_2 & \bar{Q}_{45}H_2 & \bar{Q}_{44}H_4 & \bar{Q}_{45}H_4 \\ & \bar{Q}_{55}H_1 & \bar{Q}_{45}H_3 & \bar{Q}_{55}H_3 & \bar{Q}_{45}H_2 & \bar{Q}_{55}H_2 & \bar{Q}_{45}H_4 & \bar{Q}_{55}H_4 \\ & & \bar{Q}_{44}H_5 & \bar{Q}_{45}H_5 & \bar{Q}_{44}H_4 & \bar{Q}_{45}H_4 & \bar{Q}_{44}H_6 & \bar{Q}_{45}H_6 \\ & & & \bar{Q}_{55}H_5 & \bar{Q}_{45}H_4 & \bar{Q}_{55}H_4 & \bar{Q}_{45}H_6 & \bar{Q}_{55}H_6 \\ & & & & \bar{Q}_{44}H_3 & \bar{Q}_{45}H_3 & \bar{Q}_{44}H_5 & \bar{Q}_{45}H_5 \\ & & & & & \bar{Q}_{55}H_3 & \bar{Q}_{45}H_5 & \bar{Q}_{55}H_5 \\ & & & & & & \bar{Q}_{44}H_7 & \bar{Q}_{45}H_7 \\ & & & & & & & \bar{Q}_{55}H_7 \end{bmatrix},$$

Symmetric

For displacement model FOST

$$\mathbf{D}_m = \sum_{L=1}^{NL} \begin{bmatrix} \bar{Q}_{11}H_1 & \bar{Q}_{12}H_1 & \bar{Q}_{13}H_1 \\ \text{Symmetric} & \bar{Q}_{22}H_1 & \bar{Q}_{23}H_1 \\ & & \bar{Q}_{33}H_1 \end{bmatrix}, \quad \mathbf{D}_s = \sum_{L=1}^{NL} \begin{bmatrix} \bar{Q}_{44}H_1 & \bar{Q}_{45}H_1 & \bar{Q}_{44}H_2 & \bar{Q}_{45}H_2 \\ \bar{Q}_{55}H_1 & \bar{Q}_{45}H_2 & \bar{Q}_{44}H_3 & \bar{Q}_{45}H_3 \\ \text{Symmetric} & & & \bar{Q}_{55}H_3 \end{bmatrix}.$$

The elements of the  $\mathbf{D}_c$  and  $\mathbf{D}_b$  matrices are obtained replacing  $H_1$  by  $H_2$  and  $H_3$  respectively in the  $\mathbf{D}_m$  matrix and  $H_i = (z_{L+1}^i - z_L^i)/i$ ,  $i = 1, 2, 3$ .

### Appendix C

$\mathbf{C}'$ ,  $\Delta$  and  $\mathbf{F}$  used in Eq. (22) for various displacement models are as follows:

For displacement model HOST12

$$\Delta = (u_{omn}, v_{omn}, w_{omn}, \theta_{xmn}, \theta_{ymn}, \theta_{zmn}, u_{omn}^*, v_{omn}^*, w_{omn}^*, \theta_{xmn}^*, \theta_{ymn}^*, \theta_{zmn}^*),$$

$$\mathbf{F} = \left( \alpha N_{xT}, \beta N_{yT}, -\frac{N_{xT}}{R_x} - \frac{N_{yT}}{R_y} - q_{mn}, \alpha M_{xT}, \beta M_{yT}, -\frac{M_{xT}}{R_x} - \frac{M_{yT}}{R_y} - N_{zT}, \alpha N_{xT}^*, \beta N_{yT}^*, -\frac{N_{xT}^*}{R_x} - \frac{N_{yT}^*}{R_y} - 2M_{zT}, \alpha M_{xT}^*, \beta M_{yT}^*, -\frac{M_{xT}^*}{R_x} - \frac{M_{yT}^*}{R_y} - 3N_{zT}^* \right)^t,$$

$$C'_{11} = -\alpha^2 D_{f11} - \beta^2 D_{f33} - 2c_o \beta^2 D_{f311} - c_o^2 \beta^2 D_{f1111} - \frac{D_{s11}}{R_x^2},$$

$$C'_{12} = -\alpha\beta(D_{f12} + D_{f33} - c_o^2 D_{f1111}), \quad C'_{13} = \alpha \left( \frac{D_{f11}}{R_x} + \frac{D_{f12}}{R_y} + \frac{D_{s11}}{R_x} \right),$$

$$C'_{14} = -\alpha^2 D_{f19} - \beta^2 D_{f311} - c_o \beta^2 D_{f1111} + \frac{D_{s11}}{R_x} - \frac{D_{s15}}{R_x^2},$$

$$C'_{15} = -\alpha\beta(D_{f110} + D_{f311} + c_o D_{f1111}), \quad C'_{16} = \alpha \left( D_{f17} + \frac{D_{f19}}{R_x} + \frac{D_{f110}}{R_y} + \frac{D_{s15}}{R_x} \right),$$

$$C'_{17} = -\alpha^2 D_{f14} - \beta^2 D_{f36} - c_o \beta^2 D_{f314} - c_o \beta^2 D_{f611} - c_o^2 \beta^2 D_{f1114} - \frac{D_{s13}}{R_x^2} + \frac{2D_{s15}}{R_x},$$

$$C'_{18} = -\alpha\beta(D_{f15} + D_{f36} - c_o D_{f314} + c_o D_{f611} - c_o^2 D_{f1114}),$$

$$C'_{19} = \alpha \left( \frac{D_{f14}}{R_x} + \frac{D_{f15}}{R_y} + 2D_{f115} + \frac{D_{s13}}{R_x} \right),$$

$$C'_{110} = -\alpha^2 D_{f112} - \beta^2 D_{f314} - c_o \beta^2 D_{f1114} + \frac{3D_{s13}}{R_x} - \frac{D_{s17}}{R_x^2},$$

$$C'_{111} = -\alpha\beta(D_{f113} + D_{f314} + c_o D_{f1114}),$$

$$C'_{112} = \alpha \left( 3D_{f18} + \frac{D_{f112}}{R_x} + \frac{D_{f113}}{R_y} + \frac{D_{s17}}{R_x} \right),$$

$$C'_{22} = -\alpha^2 D_{f33} - \beta^2 D_{f22} + 2c_o \alpha^2 D_{f311} - c_o^2 \alpha^2 D_{f1111} - \frac{D_{s22}}{R_y^2},$$

$$C'_{23} = \beta \left( \frac{D_{f12}}{R_x} + \frac{D_{f22}}{R_y} + \frac{D_{s22}}{R_y} \right), \quad C'_{24} = -\alpha\beta(D_{f29} + D_{f311} - c_o D_{f1111}),$$

$$C'_{25} = -\beta^2 D_{f210} - \alpha^2 D_{f311} + c_o \alpha^2 D_{f1111} + \frac{D_{s22}}{R_y} - \frac{D_{s26}}{R_y^2},$$

$$C'_{26} = \beta \left( D_{f27} + \frac{D_{f29}}{R_x} + \frac{D_{f210}}{R_y} + \frac{D_{s26}}{R_y} \right),$$

$$C'_{27} = -\alpha\beta(D_{f24} + D_{f36} + c_o D_{f314} - c_o D_{f611} - c_o^2 D_{f1114}),$$

$$C'_{28} = -\beta^2 D_{f25} - \alpha^2 D_{f36} + c_o \alpha^2 D_{f314} + c_o \alpha^2 D_{f611} - c_o^2 \alpha^2 D_{f1114} - \frac{D_{s24}}{R_y^2} + \frac{2D_{s26}}{R_y},$$

$$\begin{aligned}
C'_{29} &= \beta \left( \frac{D_{f24}}{R_x} + \frac{D_{f25}}{R_y} + 2D_{f215} + \frac{D_{s24}}{R_y} \right), \\
C'_{210} &= -\alpha\beta(D_{f212} + D_{f314} - c_o D_{f1114}), \\
C'_{211} &= -\beta^2 D_{f213} - \alpha^2 D_{f314} + c_o \alpha^2 D_{f1114} + \frac{3D_{s24}}{R_y} - \frac{D_{s28}}{R_y^2}, \\
C'_{212} &= \beta \left( 3D_{f28} + \frac{D_{f212}}{R_x} + \frac{D_{f213}}{R_y} + \frac{D_{s28}}{R_y} \right), \\
C'_{33} &= -\alpha^2 D_{s11} - \beta^2 D_{s22} - \frac{D_{f11}}{R_x^2} - \frac{2D_{f12}}{R_x R_y} - \frac{D_{f22}}{R_y^2}, \\
C'_{34} &= \alpha \left( \frac{D_{f19}}{R_x} + \frac{D_{f29}}{R_y} - D_{s11} + \frac{D_{s15}}{R_x} \right), \quad C'_{35} = \beta \left( \frac{D_{f110}}{R_x} + \frac{D_{f210}}{R_y} - D_{s22} + \frac{D_{s26}}{R_y} \right), \\
C'_{36} &= -\alpha^2 D_{s15} - \beta^2 D_{s26} - \frac{D_{17}}{R_x} - \frac{D_{19}}{R_x^2} - \frac{D_{110}}{R_x R_y} - \frac{D_{27}}{R_y} - \frac{D_{29}}{R_x R_y} - \frac{D_{210}}{R_y^2}, \\
C'_{37} &= \alpha \left( \frac{D_{f14}}{R_x} + \frac{D_{f24}}{R_y} + \frac{D_{s13}}{R_x} - 2D_{s15} \right), \quad C'_{38} = \beta \left( \frac{D_{f15}}{R_x} + \frac{D_{f25}}{R_y} + \frac{D_{s24}}{R_y} - 2D_{s26} \right), \\
C'_{39} &= -\frac{D_{f14}}{R_x^2} - \frac{D_{f15}}{R_x R_y} - \frac{2D_{f115}}{R_x} - \frac{D_{f24}}{R_x R_y} - \frac{D_{f25}}{R_y^2} - \frac{2D_{f215}}{R_y} - \alpha^2 D_{s13} - \beta^2 D_{s24}, \\
C'_{310} &= \alpha \left( \frac{D_{f112}}{R_x} + \frac{D_{f212}}{R_y} - 3D_{s13} + \frac{D_{s17}}{R_x} \right), \quad C'_{311} = \beta \left( \frac{D_{f113}}{R_x} + \frac{D_{f213}}{R_y} - 3D_{s24} + \frac{D_{s28}}{R_y} \right), \\
C'_{312} &= -\frac{D_{f112}}{R_x^2} - \frac{3D_{f18}}{R_x} - \frac{3D_{f28}}{R_y} - \frac{D_{f113}}{R_x R_y} - \frac{D_{f212}}{R_x R_y} - \frac{D_{f213}}{R_y^2} - \alpha^2 D_{s17} - \beta^2 D_{s28}, \\
C'_{44} &= -\alpha^2 D_{f99} - \beta^2 D_{f1111} - D_{s11} + \frac{2D_{s15}}{R_x} - \frac{D_{s55}}{R_x^2}, \\
C'_{45} &= -\alpha\beta(D_{f910} + D_{f1111}), \quad C'_{46} = \alpha \left( D_{f79} + \frac{D_{f99}}{R_x} + \frac{D_{f910}}{R_y} - D_{s15} + \frac{D_{s55}}{R_x} \right), \\
C'_{47} &= -\alpha^2 D_{f49} - \beta^2 D_{f611} - c_o \beta^2 D_{f1114} + \frac{D_{s13}}{R_x} - 2D_{s15} - \frac{D_{s35}}{R_x^2} + \frac{2D_{s55}}{R_x}, \\
C'_{48} &= -\alpha\beta(D_{f59} + D_{f611} - c_o D_{f1114}), \quad C'_{49} = \alpha \left( \frac{D_{f49}}{R_x} + \frac{D_{f59}}{R_y} + 2D_{f915} + D_{s13} + \frac{D_{s35}}{R_x} \right), \\
C'_{410} &= -\alpha^2 D_{f912} - \beta^2 D_{f1114} - 3D_{s13} + \frac{D_{s17}}{R_x} + \frac{3D_{s35}}{R_x} - \frac{D_{s57}}{R_x^2}, \\
C'_{411} &= -\alpha\beta(D_{f913} + D_{f1114}), \quad C'_{412} = \alpha \left( 3D_{f89} + \frac{D_{f912}}{R_x} + \frac{D_{f913}}{R_y} - D_{s17} + \frac{D_{s57}}{R_x} \right), \\
C'_{55} &= -\beta^2 D_{f1010} - \alpha^2 D_{f1111} - D_{s22} + \frac{2D_{s26}}{R_y} - \frac{D_{s66}}{R_y^2}, \\
C'_{56} &= \beta \left( D_{f710} + \frac{D_{f910}}{R_x} + \frac{D_{f1010}}{R_y} - D_{s26} + \frac{D_{s66}}{R_y} \right), \\
C'_{57} &= -\alpha\beta(D_{f410} + D_{f611} + c_o D_{f1114}), \\
C'_{58} &= -\beta^2 D_{f510} - \alpha^2 D_{f611} + c_o \alpha^2 D_{f1114} + \frac{D_{s24}}{R_y} - 2D_{s26} - \frac{D_{s46}}{R_y^2} + \frac{2D_{s66}}{R_y}, \\
C'_{59} &= \beta \left( \frac{D_{f410}}{R_x} + \frac{D_{f510}}{R_y} + 2D_{f1015} - D_{s24} + \frac{D_{s46}}{R_y} \right), \\
C'_{510} &= -\alpha\beta(D_{f1012} + D_{f1114}),
\end{aligned}$$

$$\begin{aligned}
C'_{511} &= -\beta^2 D_{f1013} - \alpha^2 D_{f1114} - 3D_{s24} + \frac{D_{s28}}{R_y} + \frac{3D_{s46}}{R_y} - \frac{D_{s68}}{R_y^2}, \\
C'_{512} &= \beta \left( 3D_{f810} + \frac{D_{f1012}}{R_x} + \frac{D_{f1013}}{R_y} - D_{s28} + \frac{D_{s687}}{R_y} \right), \\
C'_{66} &= -\alpha^2 D_{s55} - \beta^2 D_{s66} - \frac{D_{f99}}{R_x^2} - \frac{2D_{f910}}{R_x R_y} - \frac{D_{f1010}}{R_y^2} - D_{77} - \frac{2D_{79}}{R_x} - \frac{2D_{710}}{R_y}, \\
C'_{67} &= \alpha \left( \frac{D_{s35}}{R_x} - 2D_{s55} + \frac{D_{f49}}{R_x} + \frac{D_{f410}}{R_y} + D_{f47} \right), \\
C'_{68} &= \beta \left( \frac{D_{s46}}{R_y} - 2D_{s66} + \frac{D_{f59}}{R_x} + \frac{D_{f510}}{R_y} + D_{f57} \right), \\
C'_{69} &= -\alpha^2 D_{s35} - \beta^2 D_{s46} - \frac{D_{f49}}{R_x^2} - \frac{D_{f59}}{R_x R_y} - \frac{2D_{f915}}{R_x} - \frac{D_{f410}}{R_x R_y} - \frac{D_{f510}}{R_y^2} - \frac{2D_{f1015}}{R_y} - \frac{D_{f47}}{R_x} - \frac{D_{f57}}{R_y} - 2D_{f715}, \\
C'_{610} &= \alpha \left( -3D_{s35} + \frac{D_{s57}}{R_x} + \frac{D_{f912}}{R_x} + \frac{D_{f1012}}{R_y} + D_{f712} \right), \\
C'_{611} &= \beta \left( -3D_{s46} + \frac{D_{s68}}{R_y} + \frac{D_{f913}}{R_x} + \frac{D_{f1013}}{R_y} + D_{f713} \right), \\
C'_{612} &= -\alpha^2 D_{s57} - \beta^2 D_{s68} - \frac{3D_{f89}}{R_x} - \frac{D_{f912}}{R_x^2} - \frac{D_{f913}}{R_x R_y} - \frac{3D_{f810}}{R_y} - \frac{D_{f1012}}{R_x R_y} - \frac{D_{f1013}}{R_y^2} - 3D_{f78} - \frac{D_{f712}}{R_x} - \frac{D_{f713}}{R_y}, \\
C'_{77} &= -\alpha^2 D_{f44} - \beta^2 D_{f66} - 2c_o \beta^2 D_{f614} - c_o^2 \beta^2 D_{f1414} - \frac{D_{s33}}{R_x^2} + \frac{4D_{s35}}{R_x} - 4D_{s55}, \\
C'_{78} &= -\alpha \beta (D_{f45} + D_{f66} - c_o^2 D_{f1414}), \quad C'_{79} = \alpha \left( \frac{D_{f44}}{R_x} + \frac{D_{f45}}{R_y} + 2D_{f415} - 2D_{s35} + \frac{D_{s33}}{R_x} \right), \\
C'_{710} &= -\alpha^2 D_{f412} - \beta^2 (D_{f614} + c_o D_{f1414}) - 6D_{s35} + \frac{2D_{s57}}{R_x} + \frac{3D_{s33}}{R_x} - \frac{D_{s37}}{R_x^2}, \\
C'_{711} &= -\alpha \beta (D_{f413} + D_{f614} + c_o D_{f1414}), \quad C'_{712} = \alpha \left( 3D_{f48} + \frac{D_{f412}}{R_x} + \frac{D_{f413}}{R_y} - 2D_{s57} + \frac{D_{s37}}{R_x} \right), \\
C'_{88} &= -\alpha^2 D_{f66} - \beta^2 D_{f55} + 2c_o \alpha^2 D_{f614} - c_o^2 \alpha^2 D_{f1414} - \frac{D_{s44}}{R_y^2} + \frac{4D_{s46}}{R_y} - 4D_{s66}, \\
C'_{89} &= \beta \left( \frac{D_{f45}}{R_x} + \frac{D_{f55}}{R_y} + 2D_{f515} - 2D_{s46} + \frac{D_{s44}}{R_y} \right), \quad C'_{810} = -\alpha \beta (D_{f512} + D_{f614} - c_o D_{f1414}), \\
C'_{811} &= -\beta^2 D_{f513} - \alpha^2 (D_{f614} - c_o D_{f1414}) - 6D_{s46} + \frac{2D_{s68}}{R_y} + \frac{3D_{s44}}{R_y} - \frac{D_{s48}}{R_y^2}, \\
C'_{812} &= \beta \left( 3D_{f58} + \frac{D_{f512}}{R_x} + \frac{D_{f513}}{R_y} - 2D_{s68} + \frac{D_{s48}}{R_y} \right), \\
C'_{99} &= -\alpha^2 D_{s33} - \beta^2 D_{s44} - \frac{D_{f44}}{R_x^2} - \frac{D_{f55}}{R_y^2} - \frac{2D_{f45}}{R_x R_y} - \frac{4D_{f415}}{R_x} - \frac{4D_{f515}}{R_y} - 4D_{f1515}, \\
C'_{910} &= \alpha \left( -3D_{s33} + \frac{D_{s37}}{R_x} + \frac{D_{f412}}{R_x} + \frac{D_{f512}}{R_y} + 2D_{f1215} \right), \\
C'_{911} &= \beta \left( -3D_{s44} + \frac{D_{s48}}{R_y} - \frac{D_{f413}}{R_x} + \frac{D_{f513}}{R_y} + 2D_{f1315} \right), \\
C'_{912} &= -\alpha^2 D_{s37} - \beta^2 D_{s48} - \frac{3D_{f48}}{R_x} - \frac{D_{f412}}{R_x^2} - \frac{D_{f513}}{R_y^2} - \frac{D_{f413}}{R_x R_y} - \frac{3D_{f58}}{R_y} - \frac{D_{f512}}{R_x R_y} - 6D_{f815} - \frac{2D_{f1215}}{R_x} - \frac{2D_{f1315}}{R_y}, \\
C'_{1010} &= -\alpha^2 D_{f1212} - \beta^2 D_{f1414} - 9D_{s33} + \frac{6D_{s37}}{R_x} - \frac{D_{s77}}{R_x^2},
\end{aligned}$$



$$\begin{aligned}
C'_{1011} &= -\alpha\beta(D_{f1213} + D_{f1414}), & C'_{1012} &= \alpha\left(3D_{f812} + \frac{D_{f1212}}{R_x} + \frac{D_{f1213}}{R_y} - 3D_{s37} + \frac{D_{s77}}{R_x}\right), \\
C'_{1111} &= -\alpha^2 D_{f1414} - \beta^2 D_{f1313} + \frac{6D_{s48}}{R_y} - \frac{D_{s88}}{R_y^2} - 9D_{s44}, \\
C'_{1112} &= \beta\left(3D_{f813} + \frac{D_{f1213}}{R_x} + \frac{D_{f1313}}{R_y} + \frac{D_{s88}}{R_y} - 3D_{s48}\right), \\
C'_{1212} &= -\alpha^2 D_{s77} - \beta^2 D_{s88} - 9D_{f88} - \frac{6D_{f812}}{R_x} - \frac{6D_{f813}}{R_y} - \frac{D_{f1212}}{R_x^2} - \frac{2D_{f1213}}{R_x R_y} - \frac{D_{f1313}}{R_y^2}, \\
C'_{ij} &= C'_{ji}, \quad i, j = 1 \text{ to } 12.
\end{aligned}$$

For displacement model HOST11

$$\begin{aligned}
\mathbf{A} &= (u_{omn}, v_{omn}, w_{omn}, \theta_{xmn}, \theta_{ymn}, \theta_{zmn}, u_{omn}^*, v_{omn}^*, w_{omn}^*, \theta_{xmn}^*, \theta_{ymn}^*), \\
\mathbf{F} &= \left( \alpha N_{xT}, \beta N_{yT}, -\frac{N_{xT}}{R_x} - \frac{N_{yT}}{R_y} - q_{mn}, \alpha M_{xT}, \beta M_{yT}, -\frac{M_{xT}}{R_x} - \frac{M_{yT}}{R_y} - N_{zT}, \alpha N_{xT}^*, \beta N_{yT}^*, -\frac{N_{xT}^*}{R_x} - \frac{N_{yT}^*}{R_y} \right. \\
&\quad \left. - 2M_{zT}, \alpha M_{xT}^*, \beta M_{yT}^* \right)^t.
\end{aligned}$$

The elements of  $\mathbf{C}'$  matrix for this displacement model can be obtained by eliminating the twelfth row and twelfth column of  $\mathbf{C}'$  matrix of the displacement model HOST12.

For displacement model HOST9

$$\begin{aligned}
\mathbf{A} &= (u_{omn}, v_{omn}, w_{omn}, \theta_{xmn}, \theta_{ymn}, u_{omn}^*, v_{omn}^*, \theta_{xmn}^*, \theta_{ymn}^*), \\
\mathbf{F} &= \left( \alpha N_{xT}, \beta N_{yT}, -\frac{N_{xT}}{R_x} - \frac{N_{yT}}{R_y} - q_{mn}, \alpha M_{xT}, \beta M_{yT}, \alpha N_{xT}^*, \beta N_{yT}^*, \alpha M_{xT}^*, \beta M_{yT}^* \right)^t, \\
C'_{11} &= -\alpha^2 D_{f11} - \beta^2 D_{f33} - 2c_o \beta^2 D_{f39} - c_o^2 \beta^2 D_{f99} - \frac{D_{s11}}{R_x^2}, \\
C'_{12} &= -\alpha\beta(D_{f12} + D_{f33} - c_o^2 D_{f99}), & C'_{13} &= \alpha\left(\frac{D_{f11}}{R_x} + \frac{D_{f12}}{R_y} + \frac{D_{s11}}{R_x}\right), \\
C'_{14} &= -\alpha^2 D_{f17} - \beta^2 D_{f39} - c_o \beta^2 D_{f99} + \frac{D_{s11}}{R_x} - \frac{D_{s15}}{R_x^2}, \\
C'_{15} &= -\alpha\beta(D_{f18} + D_{f39} + c_o D_{f99}), \\
C'_{16} &= -\alpha^2 D_{f14} - \beta^2 D_{f36} - c_o \beta^2 D_{f312} - c_o \beta^2 D_{f69} - c_o^2 \beta^2 D_{f912} - \frac{D_{s13}}{R_x^2} + \frac{2D_{s15}}{R_x}, \\
C'_{17} &= -\alpha\beta(D_{f15} + D_{f36} - c_o D_{f312} + c_o D_{f69} - c_o^2 D_{f912}), \\
C'_{18} &= -\alpha^2 D_{f110} - \beta^2 D_{f312} - c_o \beta^2 D_{f912} + \frac{3D_{s13}}{R_x} - \frac{D_{s17}}{R_x^2}, \\
C'_{19} &= -\alpha\beta(D_{f111} + D_{f312} + c_o D_{f912}), \\
C'_{22} &= -\alpha^2 D_{f33} - \beta^2 D_{f22} + 2c_o \alpha^2 D_{f39} - c_o^2 \alpha^2 D_{f99} - \frac{D_{s22}}{R_y^2}, \\
C'_{23} &= \beta\left(\frac{D_{f12}}{R_x} + \frac{D_{f22}}{R_y} + \frac{D_{s22}}{R_y}\right), & C'_{24} &= -\alpha\beta(D_{f27} + D_{f39} - c_o D_{f99}), \\
C'_{25} &= -\beta^2 D_{f28} - \alpha^2 D_{f39} + c_o \alpha^2 D_{f99} + \frac{D_{s22}}{R_y} - \frac{D_{s26}}{R_y^2}, \\
C'_{26} &= -\alpha\beta(D_{f24} + D_{f36} + c_o D_{f312} - c_o D_{f69} - c_o^2 D_{f912}), \\
C'_{27} &= -\beta^2 D_{f25} - \alpha^2 D_{f36} + c_o \alpha^2 D_{f312} + c_o \alpha^2 D_{f69} - c_o^2 \alpha^2 D_{f912} - \frac{D_{s24}}{R_y^2} + \frac{2D_{s26}}{R_y}, \\
C'_{28} &= -\alpha\beta(D_{f210} + D_{f312} - c_o D_{f912}),
\end{aligned}$$

$$\begin{aligned}
C'_{29} &= -\beta^2 D_{f211} - \alpha^2 D_{f312} + c_o \alpha^2 D_{f912} + \frac{3D_{s24}}{R_y} - \frac{D_{s28}}{R_y^2}, \\
C'_{33} &= -\alpha^2 D_{s11} - \beta^2 D_{s22} - \frac{D_{f11}}{R_x^2} - \frac{2D_{f12}}{R_x R_y} - \frac{D_{f22}}{R_y^2}, \\
C'_{34} &= \alpha \left( \frac{D_{f17}}{R_x} + \frac{D_{f27}}{R_y} - D_{s11} + \frac{D_{s15}}{R_x} \right), & C'_{35} &= \beta \left( \frac{D_{f18}}{R_x} + \frac{D_{f28}}{R_y} - D_{s22} + \frac{D_{s26}}{R_y} \right), \\
C'_{36} &= \alpha \left( \frac{D_{f14}}{R_x} + \frac{D_{f24}}{R_y} + \frac{D_{s13}}{R_x} - 2D_{s15} \right), & C'_{37} &= \beta \left( \frac{D_{f15}}{R_x} + \frac{D_{f25}}{R_y} + \frac{D_{s24}}{R_y} - 2D_{s26} \right), \\
C'_{38} &= \alpha \left( \frac{D_{f110}}{R_x} + \frac{D_{f210}}{R_y} - 3D_{s13} + \frac{D_{s17}}{R_x} \right), & C'_{39} &= \beta \left( \frac{D_{f111}}{R_x} + \frac{D_{f211}}{R_y} - 3D_{s24} + \frac{D_{s28}}{R_y} \right), \\
C'_{44} &= -\alpha^2 D_{f77} - \beta^2 D_{f99} - D_{s11} + \frac{2D_{s15}}{R_x} - \frac{D_{s55}}{R_x^2}, & C'_{45} &= -\alpha\beta(D_{f78} + D_{f99}), \\
C'_{46} &= -\alpha^2 D_{f47} - \beta^2 D_{f69} - c_o \beta^2 D_{f912} + \frac{D_{s13}}{R_x} - 2D_{s15} - \frac{D_{s35}}{R_x^2} + \frac{2D_{s55}}{R_x}, \\
C'_{47} &= -\alpha\beta(D_{f57} + D_{f69} - c_o D_{f912}), \\
C'_{48} &= -\alpha^2 D_{f710} - \beta^2 D_{f912} - 3D_{s13} + \frac{D_{s17}}{R_x} + \frac{3D_{s35}}{R_x} - \frac{D_{s57}}{R_x^2}, \\
C'_{49} &= -\alpha\beta(D_{f711} + D_{f912}), \\
C'_{55} &= -\beta^2 D_{f88} - \alpha^2 D_{f99} - D_{s22} + \frac{2D_{s26}}{R_y} - \frac{D_{s66}}{R_y^2}, \\
C'_{56} &= -\alpha\beta(D_{f48} + D_{f69} + c_o D_{f912}), \\
C'_{57} &= -\beta^2 D_{f58} - \alpha^2 D_{f69} + c_o \alpha^2 D_{f912} + \frac{D_{s24}}{R_y} - 2D_{s26} - \frac{D_{s46}}{R_y^2} + \frac{2D_{s66}}{R_y}, \\
C'_{58} &= -\alpha\beta(D_{f810} + D_{f912}), \\
C'_{59} &= -\beta^2 D_{f811} - \alpha^2 D_{f912} - 3D_{s24} + \frac{D_{s28}}{R_y} + \frac{3D_{s46}}{R_y} - \frac{D_{s68}}{R_y^2}, \\
C'_{66} &= -\alpha^2 D_{f44} - \beta^2 D_{f66} - 2c_o \beta^2 D_{f612} - c_o^2 \beta^2 D_{f1212} - \frac{D_{s33}}{R_x^2} + \frac{4D_{s35}}{R_x} - 4D_{s55}, \\
C'_{67} &= -\alpha\beta(D_{f45} + D_{f66} - c_o^2 D_{f1212}), \\
C'_{68} &= -\alpha^2 D_{f410} - \beta^2 (D_{f612} + c_o D_{f1212}) - 6D_{s35} + \frac{2D_{s57}}{R_x} + \frac{3D_{s33}}{R_x} - \frac{D_{s37}}{R_x^2}, \\
C'_{69} &= -\alpha\beta(D_{f411} + D_{f612} + c_o D_{f1212}), \\
C'_{77} &= -\alpha^2 D_{f66} - \beta^2 D_{f55} + 2c_o \alpha^2 D_{f612} - c_o^2 \alpha^2 D_{f1212} - \frac{D_{s44}}{R_y^2} + \frac{4D_{s46}}{R_y} - 4D_{s66}, \\
C'_{78} &= -\alpha\beta(D_{f510} + D_{f612} - c_o D_{f1212}), \\
C'_{79} &= -\beta^2 D_{f511} - \alpha^2 (D_{f612} - c_o D_{f1212}) - 6D_{s46} + \frac{2D_{s68}}{R_y} + \frac{3D_{s44}}{R_y} - \frac{D_{s48}}{R_y^2}, \\
C'_{88} &= -\alpha^2 D_{f1010} - \beta^2 D_{f1212} - 9D_{s33} + \frac{6D_{s37}}{R_x} - \frac{D_{s77}}{R_x^2}, \\
C'_{89} &= -\alpha\beta(D_{f1011} + D_{f1212}), \\
C'_{99} &= -\alpha^2 D_{f1212} - \beta^2 D_{f1111} + \frac{6D_{s48}}{R_y} - \frac{D_{s88}}{R_y^2} - 9D_{s44}, \\
C'_{ij} &= C'_{ji}, \quad i, j = 1 \text{ to } 9.
\end{aligned}$$

For displacement model FOST

$$A = (u_{omn}, v_{omn}, w_{omn}, \theta_{xmn}, \theta_{ymn}),$$

$$\mathbf{F}' = \left( \alpha N_{xT}, \beta N_{yT}, -\frac{N_{xT}}{R_x} - \frac{N_{yT}}{R_y} - q_{mn}, \alpha M_{xT}, \beta M_{yT} \right)^t,$$

$$C'_{11} = -\alpha^2 D_{f11} - \beta^2 D_{f33} - 2c_o \beta^2 D_{f36} - c_o^2 \beta^2 D_{f66} - \frac{D_{s11}}{R_x^2},$$

$$C'_{12} = -\alpha\beta(D_{f12} + D_{f33} - c_o^2 D_{f66}), \quad C'_{13} = \alpha \left( \frac{D_{f11}}{R_x} + \frac{D_{f12}}{R_y} + \frac{D_{s11}}{R_x} \right),$$

$$C'_{14} = -\alpha^2 D_{f14} - \beta^2 D_{f36} - c_o \beta^2 D_{f66} + \frac{D_{s11}}{R_x} - \frac{D_{s13}}{R_x^2},$$

$$C'_{15} = -\alpha\beta(D_{f15} + D_{f36} + c_o D_{f66}),$$

$$C'_{22} = -\alpha^2 D_{f33} - \beta^2 D_{f22} + 2c_o \alpha^2 D_{f36} - c_o^2 \alpha^2 D_{f66} - \frac{D_{s22}}{R_y^2},$$

$$C'_{23} = \beta \left( \frac{D_{f12}}{R_x} + \frac{D_{f22}}{R_y} + \frac{D_{s22}}{R_y} \right), \quad C'_{24} = -\alpha\beta(D_{f24} + D_{f36} - c_o D_{f66}),$$

$$C'_{25} = -\beta^2 D_{f25} - \alpha^2 D_{f36} + c_o \alpha^2 D_{f66} + \frac{D_{s22}}{R_y} - \frac{D_{s24}}{R_y^2},$$

$$C'_{33} = -\alpha^2 D_{s11} - \beta^2 D_{s22} - \frac{D_{f11}}{R_x^2} - \frac{2D_{f12}}{R_x R_y} - \frac{D_{f22}}{R_y^2},$$

$$C'_{34} = \alpha \left( \frac{D_{f14}}{R_x} + \frac{D_{f24}}{R_y} - D_{s11} + \frac{D_{s13}}{R_x} \right), \quad C'_{35} = \beta \left( \frac{D_{f15}}{R_x} + \frac{D_{f25}}{R_y} - D_{s22} + \frac{D_{s24}}{R_y} \right),$$

$$C'_{44} = -\alpha^2 D_{f44} - \beta^2 D_{f66} - D_{s11} + \frac{2D_{s13}}{R_x} - \frac{D_{s33}}{R_x^2},$$

$$C'_{45} = -\alpha\beta(D_{f45} + D_{f66}),$$

$$C'_{55} = -\beta^2 D_{f55} - \alpha^2 D_{f66} - D_{s22} + \frac{2D_{s24}}{R_y} - \frac{D_{s44}}{R_y^2},$$

$$C'_{ij} = C'_{ji}, \quad i, j = 1 \text{ to } 5.$$

## References

- [1] Kant T, Khare RK. Finite element thermal stress analysis of composite laminates using a higher-order theory. *J Therm Stresses* 1994;17:229–55.
- [2] Khdeir AA, Reddy JN. Thermal stresses and deflections of cross-ply laminated plates using refined plate theories. *J Therm Stresses* 1991;14:419–38.
- [3] Khdeir AA, Rajab MD, Reddy JN. Thermal effects on the response of cross-ply laminated shallow shells. *Int J Solids Struct* 1992;5:653–67.
- [4] Pao YC. On higher-order theory for thermoelastic analysis of heterogeneous orthotropic cylindrical shells. In *Proceedings of Southern Conference on Theoretical and Applied Mechanics*, 6th Tampa, Fla., March 23, 24 (1972): Univ. of South Florida, 1972. p. 787–806.
- [5] Flügge W. *Stresses in shells*. New York: Springer-verlag; 1967.
- [6] Kant T. Thermal stresses in non-homogeneous shells of revolution: Theory and analysis. Tech. Rep. IIT-B/CE-79-2: Indian Institute of Technology: Bombay: Dept. of Civil Engineering; 1979.
- [7] Kant T. Thermoelasticity of thick, laminated orthotropic shells. In *Transactions of the International Conference on Structural Mechanics in Reactor Technology: Vol. M: Methods for structural analysis*: Amsterdam, Neth.: North Holland 1981.
- [8] Kant T, Patil S. Numerical results-analysis of pressures vessels using various shell theories. In *Tech. Rep. Numerical analysis of pressure vessels using various shell theories*: Indian Institute of Technology: Bombay: Dept. of Civil Engineering; 1979. p. 149–331.
- [9] Kant T. Numerical analysis of pressure vessels using various shell theories. Tech. Rep. IIT-B/CE-79-1: Indian Institute of Technology: Bombay: Dept. of Civil Engineering; 1979.
- [10] Morton SK, Webber JOH. Interlaminar failure due to mechanical and thermal stresses at the free edges of laminated plates. *Compos Sci Technol* 1993;47:1–13.
- [11] Jonnalagadda KD, Tauchert TR, Blandford GE. High-order thermoelastic composite plate theories: Analytic comparison. *J Therm Stresses* 1993;16:265–84.
- [12] He J-F. Thermoelastic analysis of laminated plates including transverse shear deformation effects. *Compos Struct* 1995;30:51–9.
- [13] Locke JE. Thermal-mechanical stress analysis of inhomogeneous antisymmetric cross-ply laminates. *Comput Struct* 1997;62(1):25–34.

- [14] Dano M-L, Hyer MW. Thermally-induced deformation behavior of unsymmetric laminates. *Int J Solids Struct* 1998;35(17):2101–20.
- [15] Ali JSM, Bhasker K, Varadan TK. A new theory for accurate thermal/mechanical flexural analysis of symmetric laminated plates. *Compos Struct* 1999;45:227–32.
- [16] Wang J, Karihaloo BL. Optimum in situ strength design of laminates under combined mechanical and thermal loads. *Compos Struct* 1999;47:635–41.
- [17] Verijenko VE, Tauchert TR, Shaikh C, Tabakov PY. Refined theory of laminated anisotropic shells for the solution of thermal stress problems. *J Therm Stresses* 1999;22:75–100.
- [18] Carrera E. An assessment of mixed and classical theories for the thermal stress analysis of orthotropic multilayered plates. *J Therm Stresses* 2000;23:797–831.
- [19] Zenkour AM, Fares ME. Thermal bending analysis of composite laminated cylindrical shells using a refined first-order theory. *J Therm Stresses* 2000;23:505–26.
- [20] Rohwer K, Rolfes R, Sparr H. Higher-order theories for thermal stresses in layered plates. *Int J Solids Struct* 2001;38:3673–87.
- [21] Patel BP, Ganapati M, Makhecha DP. Hygrothermal effects on the structural behaviour of thick composite laminates using higher-order theory. *Compos Struct* 2002;56:25–34.
- [22] Sanders JL. Jr., An improved first approximation theory for thin shells. NASA Technical Report R-24, 1959.
- [23] Cook RD. Concepts and applications of finite element analysis. New York: John Wiley and Sons; 1989.
- [24] Bhimaraddi A. Three-dimensional elasticity solution for static response of orthotropic doubly curved shallow shells on rectangular planform. *Compos Struct* 1993;24:67–77.
- [25] Pagano NJ. Exact solutions for rectangular composite and sandwich plates. *J Compos Mater* 1970;4:20–34.
- [26] Reddy TS. Three dimensional elastostatic analysis of fibre reinforced composite laminated shells. M Tech Dissertation, Department of Civil Engineering, Indian Institute of Technology Bombay, India, 1992.
- [27] Menon MP. Refined theories and finite element evaluations for multilayered composite shells. PhD Thesis, Department of Civil Engineering, Indian Institute of Technology Bombay, India, 1991.
- [28] Ren JG. Analysis of simply supported laminated circular cylindrical shells. *Compos Struct* 1989;11:277–92.